Geo-information Science and Remote Sensing

Thesis Report GIRS-2018-30

Assessing the Relation Between Peatland Vegetation Patterns and Climate Using Remote Sensing

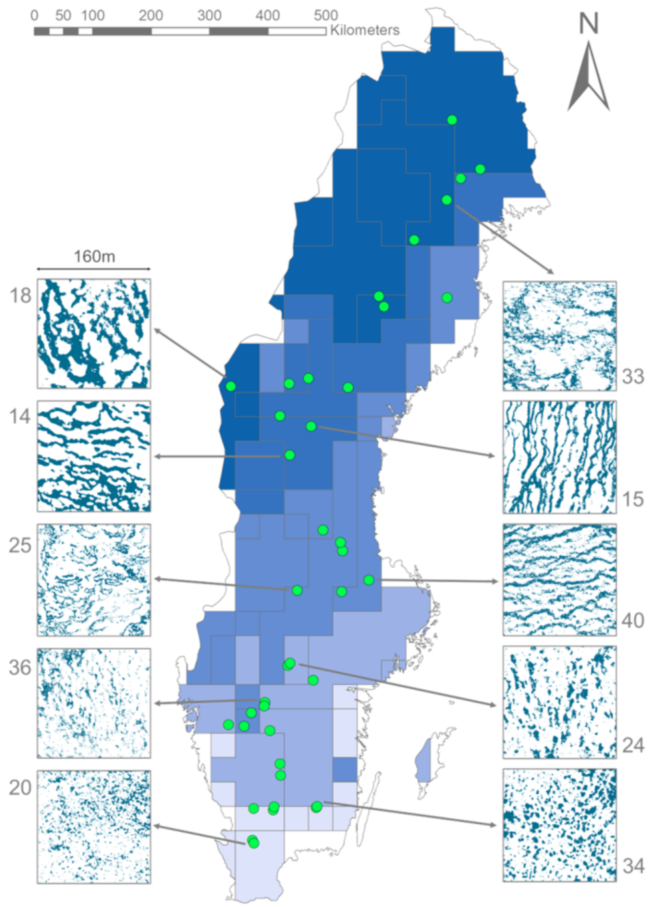

Quanxing Wan

Assessing the Relation Between Peatland Vegetation Patterns and Climate Using Remote Sensing

Author: Quanxing Wan
Registration number: 94 03 30 927 120

Supervisors:
Lammert Kooistra
Jelmer Nijp

A thesis submitted in partial fulfilment of the degree of Master of Science

at Wageningen University and Research Centre,

The Netherlands.

25-06-2018

Wageningen, The Netherlands

Thesis code number: GRS-80436

Thesis Report: GIRS-2018-30

Wageningen University and Research Centre

Laboratory of Geo-Information Science and Remote Sensing

Summary

Vegetation in boreal peatlands has long evolution periods, so it is hard to monitor considerable development of peatland vegetation patterns over a limited number of years. The objective of this research was to assess the relation between peatland vegetation change and climate development. We fell back on the nationwide climatic variability of Sweden. Temperature and precipitation gradients were referred to as the long-term climate evolution. Sweden was divided into 15 climatic sub-areas according to climatic difference. 39 sample peatlands, distributed nationwide, were determined by stratified sampling. The dynamics of hummock-hollow microform was used as the indicator of patterning change in peatland vegetation. Apart from hummock and hollow, forest, water and mud-bottom were other used classes for land-cover classification in this study. Owing to the large number of peatlands, 7 signature files from representative peatlands were applied to the rest of peatlands. The robustness of the maximum likelihood classification (MLC) for most peatland locations was acceptable. MLC inputs were RGB, IR images and digital elevation model (DEM). 1-meter buffer around sample points were generated for extracting signature profile of classes. The overall classification accuracy of representative peatlands achieved 84.35%, validated by random sample points in their own locations. According to both the visual assessment and pattern analysis (with metrics of Major, Minor and Radius of Gyration), patch size of hummocks was showing an overall decreasing trend from cold region to warm region. But, the biggest average size of hummocks among groups was witnessed in north-central region (Group 2). The metrics of Anisotropy and Minor had the highest correlations with temperature (r^2 = 0.18 and 0.12, respectively). In relation to precipitation variation, average patch area of hummocks was smaller in dryer areas. The metrics of Anisotropy and Percentage of Landscape had the strongest correlations with precipitation (r^2 = 0.14 and 0.10, respectively). Correlation between pattern metrics (of Major, Minor, Anisotropy, Percentage of Landscape and Radius of Gyration) has gone through transitions to temperature. No obvious transition occurred in correlation to precipitation. It was not evident enough to draw the conclusion that alternative stable state theory exactly applies to peatland pattern change over climatic development in Sweden. The influence of precipitation on peatland patterning needs to be taken into special consideration in follow-up studies.

Key words: Boreal peatland, hummock, hollow, pattern metrics, Maximum Likelihood Classification

Table of Contents

1 | Introduction

1.1 Context and background

Boreal peatlands are wet ecosystems which store large amounts of carbon in the form of dead plant remains, playing a significant role in the global carbon cycle (Bubier, Crill et al. 1998). Even slight changes in the water table or water temperature of peatlands may result in considerable shifts from carbon balance because of modifications in soil organic matter decay or plant production (Zhang, Li et al. 2002).

On the one hand, peatlands are “sinks” where CO_2 converge. A variety of vegetation types in peatlands can absorb carbon dioxide (CO_2) and H_2O for photosynthesis to promote carbon sequestration. On the other hand, peatlands, as an indispensable part of wetlands, emit CH_4 in large quantities, and wetlands are one of the major contributors for the CH_4 concentration in the atmosphere (Matthews and Fung 1987). Research to trace gas biogeochemistry has revealed that peatland microtopography, which refers to hummocks and hollows, is a vital driving factor of the exchange of gases for tracing carbon sequestration during the process of peat accumulation (CO_2 and CH_4) (Thomas 2003).

Many causes, such as distribution changes of peatlands, land use change from peatlands to agricultural areas (or nurturing forests) and human interferences (draining, forest removal, afforestation, peat extraction, airborne nitrogen pollution, heightened levels of atmospheric CO_2 affecting the carbon balance, etc.) have big impact on global carbon balance (Gorham 1991, Yetang and Xuetian 1997).

Generally, peatlands form through the processes of: 1) paludification; 2) formation directly on fresh, moist and non-vegetated mineral soils; 3) infilling of shallow water bodies; 4) forming on not deep basins which were occupied by early Holocene lakes (Wieder and Vitt 2006). There are many factors having remarkable impact on the functioning of peatlands. For instance, hydrology, wetness and vegetation are frequently referred to for explaining the distribution of peatlands (Breeuwer, Heijmans et al. 2008, Eppinga, Rietkerk et al. 2008, Kleinen, Brovkin et al. 2012).

Vegetation types in boreal peatlands are one of the dominant factors controlling carbon fixation, with peat mosses (bryophytes of the genus *Sphagnum*) and herbaceous plants being key species (Zhang, Li et al. 2002). Apart from that, peatland hydrology is also important for ecosystem functioning and carbon cycling (Nijp 2015). Groundwater regime in peats is highly correlated with carbon storage and fluxes (Holden 2005, Breeuwer, Heijmans et al. 2008). Biomass, transpiration of peatland vegetation, nutrient accumulation in peatland vegetation, peat accumulation and conductivity of groundwater have close interaction with each other (Kleinen, Brovkin et al. 2012). Regional hydrologic cycles will be reshaped along with climate change, contributing to the differences in water supply to peatland plants, precipitation variation, soil evaporation and plant transpiration changes and so forth. All of these changes are closely bound up with photosynthesis of peatland vegetation, thus carbon exchange is also influenced simultaneously.

Boreal peatlands show incredibly systematic patterns of small-scale topographic self-organization from the bird's eye view, such as hummock-hollow assemblages (Branfireun 2004). As shown in Figure 1.1, darker stripes are hummocks and yellowish parts are hollows. The patterned structure is believed to have potential relevance to the slow and gradual

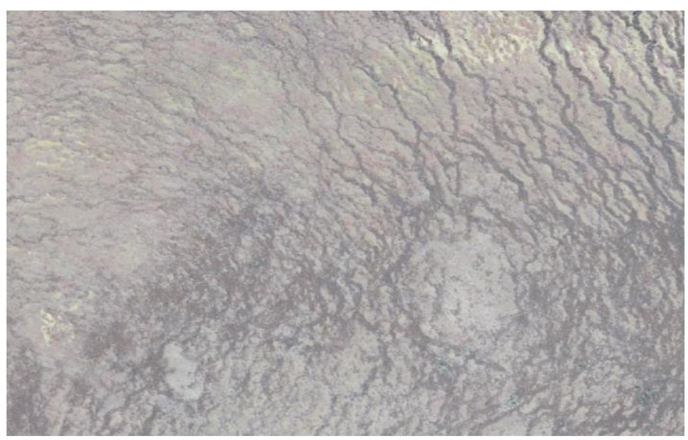

Figure 1.1. *An example of structured (elongated, highly striping) hummock-hollow patterns in Sweden (location: 60.312°N, 16.939°E)*

changes of climate and landscape (Scheffer, Carpenter et al. 2001, Rietkerk, Dekker et al. 2004). A steady increment in climate wetness has been witnessed for decades, which drove a consecutive growth of the unsaturated layer (close to surface) (Qian and Zhu 2001). That not only effectively reduced seepage loss, but also restrained peat formation (Belyea and Malmer 2004). As a consequence, a gradual decrease in carbon fixation would be observed. Different from the previous steady state consisting of homogeneous hollow, as larger spaces between hummock patterns, the ground turned into mosaics of microsites indicating wet and dry conditions, nowadays (Belyea and Malmer 2004).

Within a regional climate system, vegetation cover change is highly correlated to land-atmosphere dynamics (Shukla, Nobre et al. 1990). Speaking of peatland ecosystems, some previous research used data from field survey and meteorological observation data (online open data) to understand basic principles, which address the interaction mechanisms between peatland ecosystems and regional climate evolution (Gorham 1991).

It is also essential to derive the underlying processes for peatland response to climate change, and clarify the mechanism of peatland ecosystems' bistability, which explains the 'tipping point' behavior with the systems' resilience (Eppinga, Rietkerk et al. 2009). A relatively stable carbon uptake is modelled before the 'tipping point', and then carbon uptake amount decreases drastically after that and difficult to reverse to original conditions. Implications are disastrous.

1.2 Problem Definition

Climate development affects peatland carbon uptake and may initiate tipping points. These tipping points are so far difficult to predict. Spatial patterns of peatlands could provide insight on these tipping points. Especially, with the high availability of remote sensing products, this becomes possible now. So far, the relation between patterns and climate is untested, and it is unknown whether remote sensing may provide a solution to this problem.

Another problem exists in classifying land-cover types in peatlands with aerial imagery input. We are not going to classify all of the selected peatlands based on signature files from themselves. So, several peatlands are picked out for providing signature files for other peatland locations. However, the robustness of MLC is unknown. We suppose that it would be influenced by the consistency in color tones of different high-resolution aerial images. Besides, peatland types vary much from regions to regions. Hummock-hollow interactions present in diverse patterning characteristics and vegetation species. The acquisition time of images also influences classification robustness, because solar azimuth and illumination intensity differ between images. After going through literature, I found many studies researching on peatland patterning, based on regional scale. For instance, Holopainen and Jauhiainen (1999) were focused on peatlands in Southern Finland; Racine, Bernier et al. (2005) sampled several boreal peatland locations in Quebec (Canada), interpreted vegetation patterning by using RADARSAT-1 images. However, none of those researches used large spatial scale as this study did and they only had a few peatland locations. Thus, there was no need for them to test robustness of MLC between peatlands. I need to come up with strategies of testing robustness without reference to prior studies.

Speaking of peatland vegetation patterning change along climatic gradients, analysis conducted by Lindsay, Rigall et al. (1985) revealed that hummocks showed a upward trend in size from wetter regions to dryer regions in United Kingdom. Nevertheless, this trend may not show in Sweden, since the dominant peatland types are different between Sweden and UK. As for applying alternative stable state theory to peatland patterning change, Rietkerk, Dekker et al. (2004) showed that self-organized patchiness may exist in various ecosystems to catastrophic shifts between different states. We do not know that whether our sampling strategy is good enough for embracing "tipping points" in the process of patterning development.

1.3 Research objective and research questions

1.3.1 Research objective

The research objective is to assess the relation between peatland vegetation patterns and regional climate, based on a set of peatland locations on a climate gradient from north to south in Sweden, using a series of classified high-resolution Remote Sensing images.

1.3.2 Research questions

1) Does maximum likelihood classification show a good overall accuracy and robustness for analyzing peatland vegetation patterns from site to site?
2) How do peatland vegetation patterns change along temperature gradient in Sweden?
3) To what extent does precipitation differences influence peatland vegetation patterns?
4) Does alternative stable state theory apply to peatland pattern change over time of different locations in Sweden?

This research is relatively explorative, speaking of its broad research area, sub-area division, sampling strategy of suitable peatlands, robustness of land cover classification and interpretation of pattern metrics.

2 | Literature review

2.1 Remote Sensing and peatland researches

During the past decades from the end of 20th century, increasingly more researchers resort to remote sensing methods to broaden from on-site inspection to macroscopic regional or even global mapping and monitoring (Li, Wu et al. 2017). The broad-scale estimation of climate variables and the extraction of vegetation cover information by remote sensing technology have promoted the research progress of *land cover-climate* feedback mechanism greatly (Gaillard, Sugita et al. 2010).

Aerial photography was the firstly used remote sensing data in wetland researches (Miyamoto, Yoshino et al. 2004). Especially in the past several years, aerial photography has been increasingly more often used as a type of high spatial resolution imagery for identifying wetland vegetation types, such as applying to mangrove forest researches. Researchers tend to use it for getting clearer insights on land cover types (Guo, Li et al. 2017). However, wetland land cover classification and vegetation identification are still challenging according to the complexity of wetland landscapes, spectral confusion between different land cover types and even the impacts of biophysical variables, such as water levels, vegetation density and phenological vegetation variations (Cline, Feagin et al. 2011).

Apart from the visual interpretation techniques for wetland vegetation classification, automated classification methods (supervised classification and unsupervised classification) have also been carried out (Guo, Li et al. 2017). Unsupervised classification or clustering has already been commonly used as classification method to map wetlands and identify different vegetation types (Ozesmi and Bauer 2002). Besides, speaking of supervised classification methods, maximum likelihood classification (MLC) is most commonly resorted to. Concerning specific cases, it is even harder to classify wetlands, due to unique characteristics of wetlands at different locations (Ozesmi and Bauer 2002). The latter will make the transfer of classification models from site to the other more difficult.

The study by Rogan (2002) focused on applying various classification methods on forested ecosystems in California, the United States, where accelerated changes were undergoing due to natural and anthropogenic disturbances. Change detection is being widely used to monitor land cover changes of multiple time periods in forest management researches. Several techniques, such as Multi-temporal Tasseled Cap (Kauth-Thomas) Transformation, Multitemporal Spectral Mixture Analysis and MLC, were being used to accurately identify changes in vegetation cover of research area between 1990 and 1996. (Rogan, Franklin et al. 2002). Sharp's research team applied K-means algorithm for all cluster analyses of vegetation patterns in the study of finding relationships between water depths and submergent vegetation density in montane wetlands (Sharp, Sojda et al. 2013).

As discussed, a variety of remote sensing methods can be applied to monitor vegetation-climate dynamics of peatlands. This research chooses classification technique based on maximum likelihood algorithm, of which the theoretical basis is Bayesian classification. The classification process is combined with field inspection and sampling in the research area, reference to land resource data and high-resolution aerial images, for obtaining sufficient training samples (Dang, Jia et al. 2010). The results obtained by this maximum likelihood classification method are consistent and stable. The evaluation accuracy satisfies general observation demand of the ecological environment of peatlands.

Although some studies used aerial imagery to conduct researches of peatlands concerning different aspects, many of them were just focused on only one location. Their methods could not be directly applied to cases of other locations, owing to the untested robustness. Becker (2008) set different ground resolutions to test the effects on the calculated carbon balance of a boreal peatland "Salmisuo" in Eastern Finland. They obtained high resolution imagery taken from dirigible. After processing steps, the georectified imagery was classified into regions representing micro-site types, and used supervised classification with the maximum likelihood algorithm (Linderholm and Leine 2004).

Based on carrier data from plot-level aerial photograph interpretations, Holmström (2001) evaluated the accuracy of k nearest neighbor (kNN) estimations of Remningstorp estate in south-western Sweden, where 10% of the area are peatlands. The remote sensing data was connected with a sparse sample of field reference plots to estimate important vegetation parameters. Standing stem volume was estimated with a relatively high relative root mean square error (RMSE) of 20% at the stand level, which could be resulted from the poor quality of photographs. (Holmström, Nilsson et al. 2001)

Lehmann (2016) used an Unmanned Aerial System (UAS) to survey a pristine Sphagnum-dominated southern peat bog in Argentina. The classification procedure consisted of a multiresolution segmentation and an Object-Based Image Analysis (OBIA). Additionally, it is highly efficient to analyze high-resolution (<2 cm) CIR imagery with object-based classification techniques to classify vegetation both on species and microform level to e.g. monitoring peat bog vegetation changes. Their results show excellent overall accuracy level for species-level classification and microform-level classification, with 92% and 86% respectively (Lehmann, Münchberger et al. 2016).

Connolly (2017) integrated RS imagery with different resolutions to match specific usages within the study area of an Atlantic blanket in western Ireland. Low and medium resolution multispectral imagery were used to map the extent of peatlands. They also found that only high-resolution imagery was suitable to map sub-meter-sized linear features, such as peatland drains. For better detecting drains, they also introduced OBIA to their research (Connolly and Holden 2017).

2.2 Fold catastrophe model

The theory of catastrophic shifts in ecosystems is introduced to many researches in ecology domain. Mostly, ecosystems respond to gradual changes of climate, groundwater flow, nutrient supplying or habitat fragmentation in smooth ways, seemingly linearly and continuously with time (Fig 2.1(a)). Additionally, the status of some ecosystems could be shifted more strongly when conditions reach to a certain critical level, across a non-catastrophic threshold, due to small forcing (Fig 2.1(b)). However, after having surveys on a variety of natural ecosystems, researchers also found that abruptly drastic change, rather than smooth development, could drive some systems towards another alternative stable state. If the system is driven slightly away from the transition period of the curve, it will move to further away instead of returning back. A tiny difference, occurred in the condition, could contribute to a remarkable shift to the lower branch, with basin of attraction in the equilibrium curve skipped (Fig 2.1(c)). Another situation is that even a small perturbation could adjust the system to step over the borders of the domain of attraction when it is not far from fold bifurcation points (Fig 2.1(d)) (Scheffer, Carpenter et al. 2001, Scheffer, Bascompte et al. 2009).

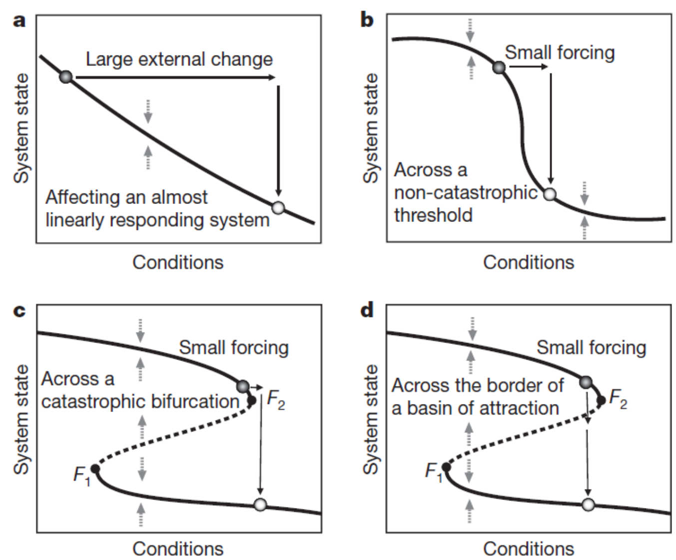

Figure 2.1. *Critical transitions in the fold catastrophe model (Scheffer, Bascompte et al. 2009)*

The mentioned fold catastrophe model has already been widely used in ecology, climate and financial market domains. Thus, it is possible to apply it to this study for interpreting peatland patterning changes.

3 | Study Area and Data Description

3.1 Study Area

The study area is located in Sweden. Choosing Sweden as the research area has the following research advantages: 1) Sweden is one of the countries with most peatlands in the world, where peatlands take up 15% of the Swedish national territory area ; 2) Latitudinal extent of Sweden is long enough to embrace a series of peatland sub-regions, classified by the dominant mire type and the distribution of specific mire types (Fig. 3.2); 3) Precipitation varies from southwestern coastal areas to eastern side, according to the extent to which it is influenced by the North Atlantic Current (CTT 2018). Besides, temperature distribution shows significant differences along the longitudinal gradient. They both contribute to the accessibility of analyzing how different climate conditions across Sweden influence peatland patterning. Most parts of Sweden receive annual precipitation between 500 mm and 800 mm (Fig. 3.1). In the south-western region, more precipitation is observed, generally between 1000 mm and 1200 mm. Most of central and northern parts are located in the rain shadow of Scandinavian Mountains. Wet air from Norwegian Sea cannot reach here, and it contributes to the dryer climate. According to the observed temperature data, for the latest 30-year period 1961-1990, the annual average temperature varies from -4.2°C (mountain peak of Tarfala) to 8.4°C (Malmo) (Fig 3.1). In this research,

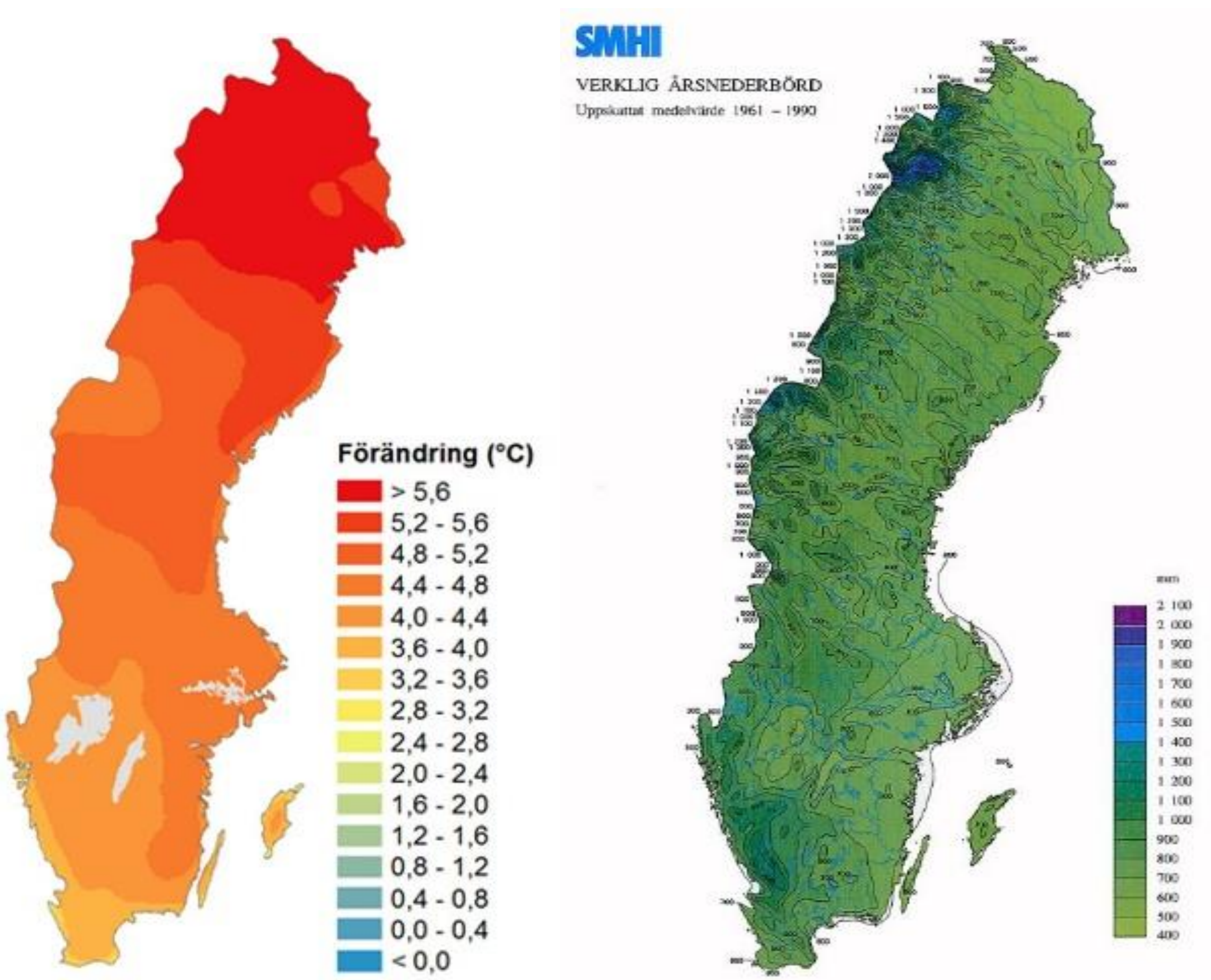

Figure 3.1. *Temperature (left) and precipitation (right) map of Sweden (Source: SMHI)*

all of the selected peatland locations are situated in the Central Aapa mire Region, Soligenous Aapa mire Region, Southern Aapa mire Region and Raised Bog mire region (Fig 3.2).

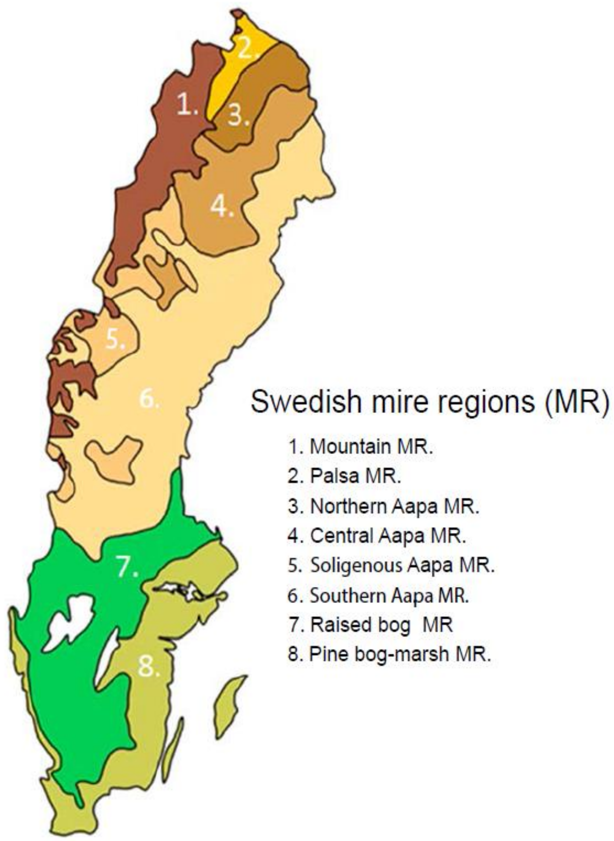

Figure 3.2. *Division of Sweden into mire regions (sub-regions of the Aapa mire included) (Gunnarsson and Löfroth 2009)*

3.2 Datasets

Several main types of spatial data were used in this study (Table 3.1), which were: 1) Raster files of high-resolution aerial photography (includes visible bands (RGB - red, blue and green) and near infrared band (Near IR)) and interpolation maps of precipitation and temperature; 2) Digital elevation model (DEM); 3) Vector maps, in which peatland distribution map and national map of Sweden are involved. All of these datasets are available from online resources. High-resolution aerial imagery and DEM can be ordered from Lantmäteriet (the Swedish mapping, cadastral and land registration authority). Other maps are freely available on the websites of Intergovernmental Panel on Climate Change (IPCC) (IPCC 2005) and European Environment Agency (EEA) (EEA 2017).

3.2.1 Remote Sensing graphic resources

1) High-resolution aerial photography

From Lantmäteriet, orthogonally projected aerial photos (orthophotos) of the entire territory of Sweden are available. In this study, orthophotos of the selected peatland locations were ordered. For both the RGB and Near IR images, the spatial resolution is 0.5 m. The size of tiles is either 5×5 km or 2.5×2.5 km, projected in the SWEREF 99 TM coordinate system. The specific acquisition time differs from site to site, which resulted from different overflight times of aircrafts through different areas. Differences of aerial photos in color tones are huge before and during the growing season. According to Markinfo (Markinfo 2006), the length of growing season in Sweden varies between 120 days in the south to 240 days in the north (~66°N), and the start date varies from May 1st to July 1st.

Among the ordered images, the image-acquisition time of all peatland locations, except 2 sites, was from May 1st to August 31st. There were no worries of most of the ordered images, since those were acquired after the specific start date of growing season in their own regions. The accurate acquisition time within a day was also provided by Lantmäteriet. Most of the images were obtained in the morning between 7:00 to 12:00, with 11% were between 12:00 to 14:30.

2) Digital elevation model

For assisting classifying land cover types in peatlands, high-resolution (2×2 m) Digital Elevation Models (DEM) were used in this study. The tiles are 2.5×2.5 km for all peatland locations. The data format was ASCII file.

3.2.2 Peatland Distribution Map

There are at least two possible selections of peatland distribution map of Sweden. One is provided by Lantmäteriet, which includes all of peatlands in Sweden (with even tiny peatlands included). It is a very suitable source, but data size is too big to process. The other source is from European Environment Agency (EEA), which includes protected peatlands in whole Europe (Natura 2000 areas) (EEA 2017). Those peatlands are normally big enough to be effectively protected by governments. In this study, the latter one was chosen as the peatland map input. The data format was in shapefile. It was clipped to the Swedish territory.

3.2.3 Meteorology data of Sweden

IPCC offers data access to climate observations with global scale only. The spatial resolution of this climate data is 25 km × 25 km. Two data formats can be selected, which are GeoTIFF and NetCDF. It is also possible to shift observation periods with different time spans. Decadal data is available for the whole 20th century (from 1901 to 2000), and 30-year data is provided from 1901 to 1990 (1901-1930, 1931-1960 and 1961-1990). For this study, monthly average precipitation and temperature data from 1961 to 1990 with GeoTIFF format was used as meteorological data input.

Table 3.1. *An overview of datasets*

Name		**Type**	**Provider**	**Data type (Spatial Resolution, if applicable)**	**Description**
National map of Sweden		Digitized maps	European Environment Agency (EEA)	Shapefile (10m reference grid)	EEA provides shapefiles of Swedish territory in different reference grids: 10m, 1km, 10km and 100km
High-resolution aerial photography	RGB	Aerial imagery	Lantmäteriet	Raster (0.5x0.5m)	A set of nationwide-covered orthophotos of Sweden
	IR	Aerial imagery	Lantmäteriet	Raster (0.5x0.5m)	
Digital elevation model (DEM)		DEM by laser scanning	Lantmäteriet	Raster (2x2m)	Acquired by using laser scanning
Peatland distribution map		Digitized maps	European Environment Agency (EEA)	Shapefile (with polygons)	Official nature reserve areas of peatlands
Interpolated precipitation maps and temperature maps		Digitized maps	Intergovernmental Panel on Climate Change (IPCC)	Raster (25x25km)	Used for filtering suitable peatland locations

4 | Methodology

4.1 An overview of methodology

The methodology for this research is divided into four main steps, which are illustrated below (Figure 4.1). Four major steps are referred to the selection of suitable peatland locations, aerial imagery and DEM preparation, supervised land-cover classification and pattern analysis. In the next section, all steps are elaborated as this flowchart indicates.

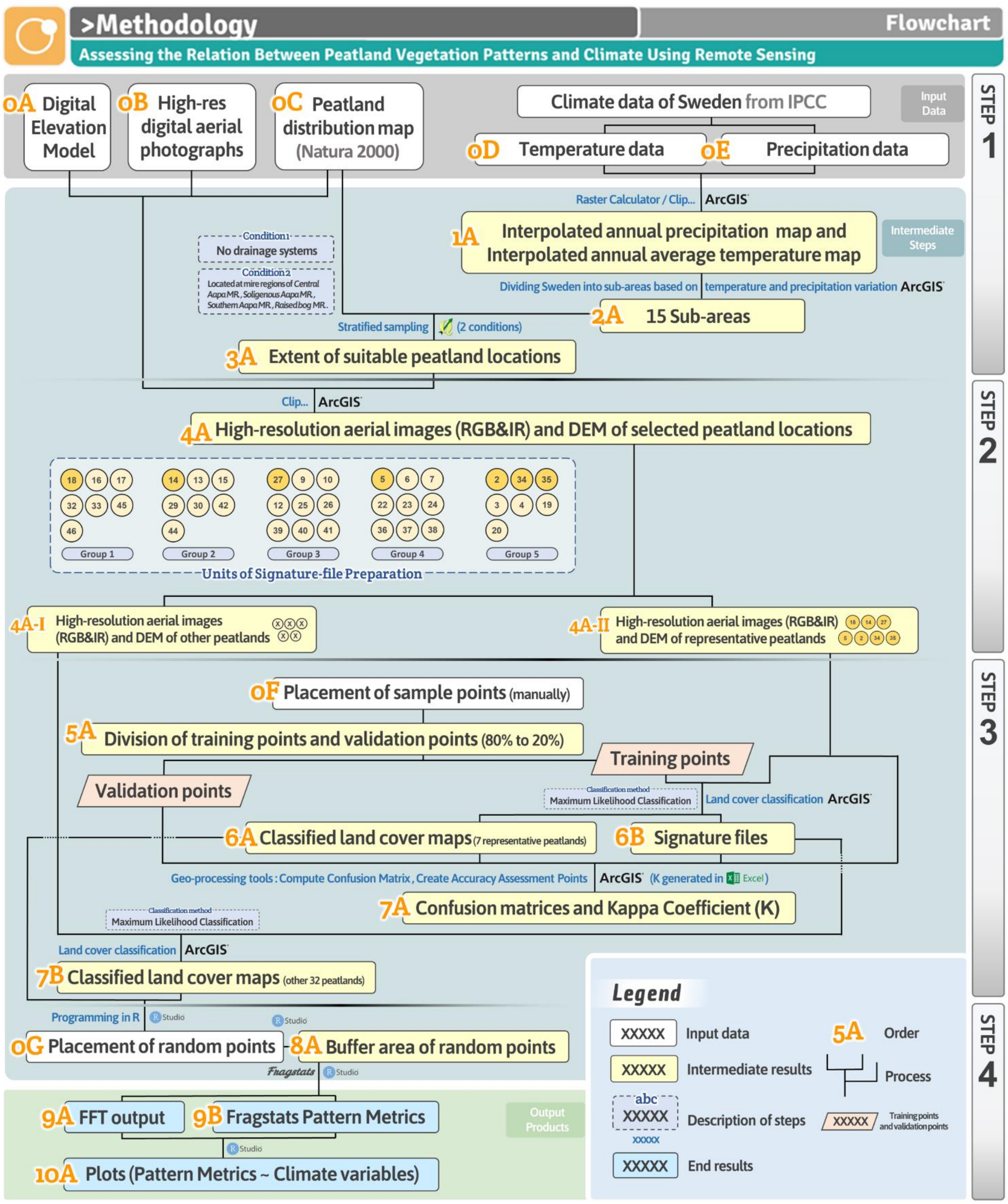

Figure 4.1. *The flow chart of methodology in this research. It includes four major step, which will be elaborated in the section 4.2.*

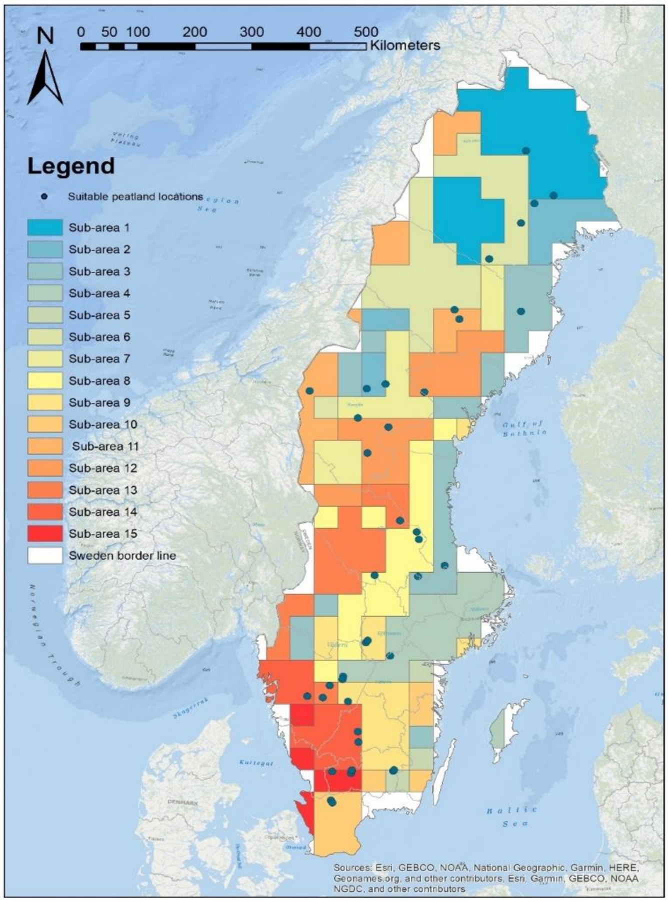

Figure 4.2. *Sub-area division in Sweden. See Table 4.1 for details on climate per sub-area*

4.2 Processing steps

To assess pattern – climate relationships, many spatial analyses needed to be carried out (Fig. 4.1). What most important was that reviling the relation between peatland vegetation patterning and climate development along climatic gradients, by adopting suitable pattern metrics. First, Sweden was divided in multiple climate zones in which patterns were classified based on aerial imagery and elevation information for 39 selected peatlands. What follows below is an elaborated description of all processing steps in the spatial analysis.

*4.2.1 **Step 1:** Selection of suitable peatland locations*

The selection method of suitable peatland locations was in compliance with the climatic gradients in Sweden. For reflecting gradients of the selected climatic factors, mean annual temperature and mean annual precipitation sum map of Sweden from IPCC were acquired (see section datasets 3.2). By integrating temperature and precipitation gradients, the whole country was divided into a series of climatic sub-areas. Data from IPCC contained maps of monthly average precipitation and temperature in 30 years from 1961 to 1990. Yearly temperature and precipitation maps were then generated after geo-processing steps with Model Builder in ArcGIS. Two main geo-processing tools were adopted: Clip and Raster Calculator (converted monthly data to yearly data). Restrained by low resolution of meteorological map inputs, it was unreasonable to divide the country into a great many sub-areas. Especially, temperature variation was not as significant as temperature along gradients. Thus, there were less precipitation sub-areas than temperature sub-areas. Being classified with quantile strategy, 3 precipitation sub-areas and 5 temperature sub-areas were produced. Next, those sub-areas were merged into 15 climatic sub-areas (Fig. 4.2) based on climate classification criteria (Table 4.1) with the tool of Raster Calculator in ArcGIS.

For reducing sampling error and showing variation in each sub-area, several peatland locations were selected as sample sites in every sub-area. The sampling extent was not whole Sweden. Coastal regions were filtered out, since the peatland age of peatlands in those regions was younger than inland peatlands due to tectonic activities. I used Buffer tool in ArcGIS for erasing areas, where the distance to coastline was nearer than 40 km. Stratified sampling based on results from previous processes was then conducted. It was realized with the ‘Stratified Sampling’ tool in the QGIS. It can be found under ‘research tools’ in ‘vector’ menu. An equal number of points (3 points) per stratum (each sub-area is a stratum in this study) were chosen. The nearest peatland to each sample point was visually paired to it and was chosen as a suitable peatland. Then, the map of Swedish mire regions (Fig 3.1) was used for checking whether those peatlands were located inside the unwanted mire regions (Mountain Mire Region, Palsa Mire Region, Northern Mire Region and Pine bog-marsh Mire Region), where permafrost peatlands, coastal peatlands were mostly found Next, polygons of selected peatlands were exported to Google Earth and visually checked whether there were drainage systems inside. In other words, the Stratified Sampling tool in QGIS was re-run over and over again until there were no peatlands inside the

Table 4.1. *An overview of sub-area classification criteria. Background colors of sub-area blocks in this chart correspond to legend of Figure 4.2. Temperature sub-areas were also groups for preparing signature files in land cover classification.*

Precipitation Sub-areas / Annual precipitation range \ Temperature Sub-areas / Annual average temperature range		Group 1	Group 2	Group 3	Group 4	Group 5
		-6.0°C 0.0°C	0.0°C 1.0°C	1.0°C 5.0°C	5.0°C 6.0°C	6.0°C 8.0°C
1	441mm 608mm	Sub-area 1 Very low temperature Low precipitation	Sub-area 2 Low temperature Low precipitation	Sub-area 3 Moderate temperature Low precipitation	Sub-area 4 High temperature Low precipitation	Sub-area 5 Very high temperature Low precipitation
2	608mm 684mm	Sub-area 6 Very low temperature Moderate precipitation	Sub-area 7 Low temperature Moderate precipitation	Sub-area 8 Moderate temperature Moderate precipitation	Sub-area 9 High temperature Moderate precipitation	Sub-area 10 Very high temperature Moderate precipitation
3	684mm 1132mm	Sub-area 11 Very low temperature High precipitation	Sub-area 12 Low temperature High precipitation	Sub-area 13 Moderate temperature High precipitation	Sub-area 14 High temperature High precipitation	Sub-area 15 Very high temperature High precipitation

unwanted mire regions and no peatlands with much human interference.

According to the selection result of suitable peatland locations, 39 peatland sites were used for conducting classification process and geostatistical analysis (with 1st order significance in Appendix A) were ensured. Their coordinates were recorded for ordering aerial imagery and DEM files (see also Appendix A).

4.2.2 *Step 2: Aerial imagery and DEM preparation*

As mentioned in 3.2, aerial images and DEM of the selected tiles were ordered from Lantmäteriet. Afterwards, all of RGB and IR images were clipped with the shapefiles of those suitable peatlands. For DEM raster files, there was an extra step. The neighboring tiles were merged by using Mosaic tool in ArcGIS, if corresponding tiles of aerial images were with the size of 5×5 km, to fit sizes of the corresponded high-resolution images.

4.2.3 *Step 3: Supervised Landcover Classification*

With peatland locations settled and required RS data prepared, supervised landcover classification was then carried out for all of the selected peatlands. Based on researcher's knowledge about peatland vegetation, sample points in each image that were representative of specific land cover types were selected and then directed the software of ArcGIS to use these training points as references for the classification of all other pixels in the images (eXtension.org 2013). The classification method of Maximum Likelihood Classification has been applied to this study. It generally produces the most accurate classification results and accounts for covariance between different bands (Booth and Oldfield 1989, Hogland, Billor et al. 2013).

Selection of representative peatlands

The peatlands fulfilling the selection requirements (Step 1) were divided into 5 groups, which were the same groups as temperature sub-areas. The individual groups for testing robustness of MLC were the same groups as temperature sub-areas. That was because temperature was a key factor influencing peatland vegetation growth. I supposed that peatland vegetation in different locations would show similar spectral signature under the same temperature conditions. However, difference in acquisition time between images was a non-negligible disturbing factor. The group-division result can be checked in Appendix A. For testing the robustness of MLC, only one peatland in each group (except from group 5 (group with very high temperature)) was selected as the representative peatland for generating signature files. The criteria for picking out representative peatlands were: 1) heterogeneity of land cover types (this peatland should include all of the land cover types defined in the study); 2) for each category, it should contain various patches showing much difference in spectral characteristics from each other; 3) similar color tone of its RGB image to that of the majority of peatlands in the same group is preferred.

Group 5 had 3 representative peatlands, which were peatland 2, peatland 34 and peatland 35, respectively. It was hard to make a choice of picking out representative peatlands from Group 5. Initially, Peatland 34 (56.823° N, 15.278°E, on the southeast of Sweden) and Peatland 35 (next to Peatland 34) were merged as an entity for generating signature file. However, its classification accuracy was terrible (see Table 5.1). Then, reasons behind were figured out. Firstly, Peatland 35 had a large area of mud-bottom in its central area, intertwined with small patches of hummocks. The MLC algorithm did not detect many of those patches. Secondly, hummocks showed in different color tones in these two peatland locations, darker in Peatland 34 and brighter in the other. Thus, it proved necessary to divide them into two individual peatlands for preparing signature files.

However, the robustness of MLC, applied to other peatlands (with signature file from Peatland 34 or Peatland 35), was then proven to be awful. Main regions of most peatlands were classified into hummocks, where those areas should be hollows. Then, I found it applicable to join Peatland 2 in the representative peatlands to classify those peatlands, where signature file from Peatland 34 or Peatland 35 performed badly. It included all of the used land cover types and it has closer color tone with other peatlands in this group. The algorithm did not make big mistakes in recognizing big patches of hollows as hummocks anymore.

Preparation of signature files

After representative peatlands were selected, the preparation of signature files could start. Signature files contain unique signature statistics for each class. Preferably, the spectral signature of representative peatlands would be consistent with that of other peatlands in the same group. Not only did peatland vegetation type influence spectral signature of hummock-hollow microform, but also factors like acquisition time within a day of images, the specific period in growing season affected.

There were 5 land cover categories being used in this study, which were hummock, hollow, water, forest and mud-bottom. Taking the workload of classification into consideration, it was feasible to classify around 5 classes. Except from hummock-hollow vegetation, mud-bottom, forest, water and sedge were the most easily-found land-cover types in the selected peatlands. However, sedge was not found in every site and would not be a disturbing factor of classifying hummock-hollow vegetation. Then, I decided to exclude it from this study. There were 105 sample points spread over each representative peatland. The number of sample points of every class was determined by their spectral differences from each other. For instance, water was the most distinguishable land cover type, then it had the least number of sample points (10 points); hummock and hollow were the most important land cover types and hard to identify from each other, so they both had the greatest number of sample points (30 points each). The training and validation ratio of sample points was set to 4:1 (80% and 20% respectively, see Figure 4.3). Training points were used for generating signature files, while validation points were used to assess the classification accuracy. Next, a square (envelope) buffer (with 10-meter radius in the first-round classification and 1-meter radius in the second-round classification; the reason of using two rounds of classification will be discussed in the following part) was created surrounding all of training points. Those buffers only contain one homogenous land cover type. If not, the MLC algorithm could get puzzled with recognizing other pixels in the same image, which would result in worse performance of land cover classification. So, the adjustment of the buffer radius from 1st round to 2nd round classification ensured that the square was small enough to fall within most of land-cover patches.

Class /Land cover type	Sample points (Training points+ Validation points)			A glimpse of the appearance of each class
	Total Amount	Training points	Validation points	
Hummock	30	24	6	
Hollow	30	24	6	
Water	10	8	2	
Forest	15	12	3	
Mud-bottom	20	16	4	
Total	**105**	**84**	**21**	

Figure 4.3. *Classification key applied to this study. It shows the amount of sample points for all classes in each signature file. With a fixed ratio of training points and validation points (4:1), the amount of training points and validation points is also shown in the figure. In the rightmost column, the examples of how classes could look like in RGB images provided. Among those classes, the distinction between hummocks and hollows is the hardest to tell. hollows are generally more yellowish and brighter, while hummocks are greyish or slightly greenish and in darker color tones. Besides, hummocks are generally more striping. Water and forest are easy to classify with very distinctive color tones. Mud-bottom presents in darker color tones than hummock and mostly aggregates in specific regions.*

In the first-round classification, signature files were generated only in representative peatland locations. Peatland 18 (close to Scandinavian Mountains in the westernmost region of Sweden, close to Storlien) stood for group 1 (group of very low temperature). Peatland 14 (in the central region, close to the lake of Svegssjön) represented group 2 (group of low temperature). Peatland 27 (on the mid-south of Sweden, close to Lake Hyn) was the representative peatland location of group 3 (group of moderate temperature). Peatland 5 (on the south of Sweden, close to Mörhult) provided signature file for group 4 (group of high temperature). Peatland 34&35 (on the southeast of Sweden, close to Lessebo N) and Peatland 2 (on the southwest, next to the lake of Torserydssjön) were picked out for group 5 (group of very high temperature). In consideration of the bad performance in land cover classification of applying signature file of Peatland 34&35 to other peatlands in group 5, I made changes in the 2nd-round classification: 1) Peatland 34 and Peatland 35 should provide separate signature files, instead of being seen as an entity; 2) test the signature files of the above-mentioned 3 peatlands in group 5 to other peatlands in this group and use the one with the best robustness.

Carry out land-cover classification

Two rounds of land cover classification were carried out for all peatlands. The second-round classification an improved version after learning a lesson from the low classification accuracy in the first-round classification. Firstly, the buffer radius of sample points decreased from 10m to 1m, as mentioned before. Secondly, more types of classification input were used. RGB image, IR image and DEM were integrated as inputs in the 2nd round, while RGB image was the only input in the 1st round. The signature result was then determined by spectral properties of aerial imagery and local elevation information, which were associated with predesignated classes of training points.

For most land cover types, those were already easy to distinguish with RGB and IR images. Telling hummocks from hollows was the most challenging part. Generally, hummocks would show similar color tones with hollows, either a bit greener or darker, in RGB images. Hollows were normally in bright color tones or yellowish color. In IR images, hummocks mostly showed in pinkish colors (high IR values due to vegetation). Compared to the color tone of neighboring forest patches, that of hummocks was brighter and more consistent from site to site. There were two major problems in classifying land cover types: 1) Sparse bushs presented in similar color tones with hummocks in IR images (see Figure 4.4); 2) Some greyish patches (in RGB images) was hard to distinguish by analyzing spectral properties in RGB and IR images, where the patches were either hummocks or mud-bottoms. For those kinds of hard-to-tell patches, DEM played an important role in identifying land cover types. Transects with elevation information, generated by the toolbar of 3D analyst in ArcGIS, definitely helped differentiating land cover types with similar color tones in aerial imagery, but different heights in DEM. Several transects were drawn in problematic areas. For problem 1, if the fluctuation of heights between unknown patches and neighboring cells in profile were big (>3m), then those patches were very likely to be forests; if not (⩽3m), then those would be highly possible to be hummocks (Figure 4.5). For problem 2, if the elevation of unknown patches was lower than neighboring cells, then those patches should be classified as mud-bottoms; if higher, then those were hummocks. The end results of Maximum Likelihood Classification (in ArcGIS) were classified land-cover maps and confidence rasters

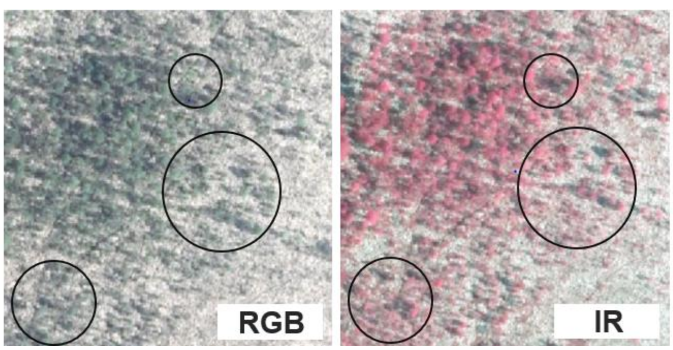

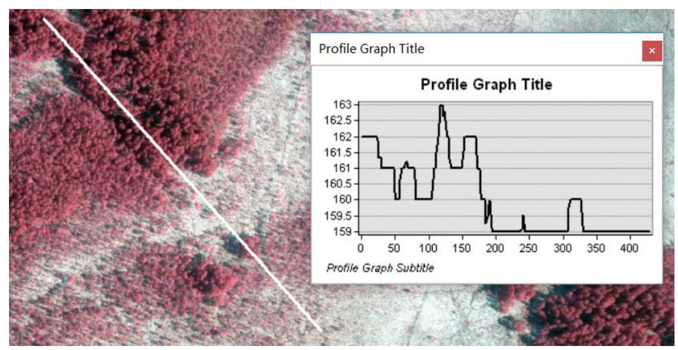

Figure 4.4. (left) *An example of areas where trees may be wrongly classified as hummocks. Green pixels in RGB image (left) and red pixels in IR image (right) are actually sparse bushes, which should have been classified as forests. However, the MLC algorithm mostly recognizes these pixels as hummocks.*

Figure 4.5. (right) *An example of generating transects by using DEM data for determining land cover types. The profile graph provides elevation information of the transect (white line) in the IR image (background image), from upper-left to bottom-right. The units of both x and y axes (of the profile) are in meters.*

Classification results of peatlands had direct impact on statistics of all pattern metrics. The goal of overall classification accuracy was set to over 70%. As for hummocks, preferably the classification accuracy should be greater than 75%. It had been set to a higher value than the overall accuracy, since only hummock patches were then derived as input for analyzing pattern metrics. If the distribution of hummocks from classified maps could not reflect the ground truth well, then the whole process of analyzing pattern metrics was meaningless.

*4.2.4 **Step 4:** Pattern Analysis*

In boreal peatlands, vegetation self-organizes into geometrically structured mosaics of patches (Eppinga, Rietkerk et al. 2008). To quantify change of vegetation patterns in peatlands, relate it to regional climate development, and clearly show the underlying resilience, the analysis of pattern metrics was indispensable.

Carry out pattern analysis

The inputs of this step were classified maps (within the extents of peatlands) from step 3 and DEM rasters from step 2. A large number of sample points were generated with equal distance to each other in peatlands. The sampling zones were in the same extent as DEM tiles. The total amount of sample points in each peatland location was set to 500 or 1000, depending on the size of peatlands. But, the number of points which actually located inside peatland scopes (map source of Natura 2000) was smaller. Fast Fourier Transform (FFT) was then computed with buffers of 20-meter radius, surrounding the above-mentioned sample points. This buffer size was suitable for analyzing hummock-hollow microforms. The output text files contained several metrics, which reflected hummocks' patterning characteristics within buffers. Among those metrics, Major, Minor and Aniso (anisotropy) were the most significant ones for this study. As can be seen in Figure 4.6, the graph on the right depicted the generalized patterning of hummocks in buffer areas, presented in the blue cluster in the center. An ellipse re-generalized patterning of the cluster. All of the generated metrics were characteristics of the ellipse actually. Major represented the length of major axis. Minor was the length of minor axis. Anisotropy denoted the aspect ratio, thus its value was always higher than 1. These metrics were all closely linked with research interests ——size and shape of hummock patches in peatlands.

The only metric in FFT output, which was not deemed important, was Angle (the angle between the major axis of ellipse and x-axis of the graph). The reason was that Angle was more related to terrain factors of aspect and slope than other metrics.

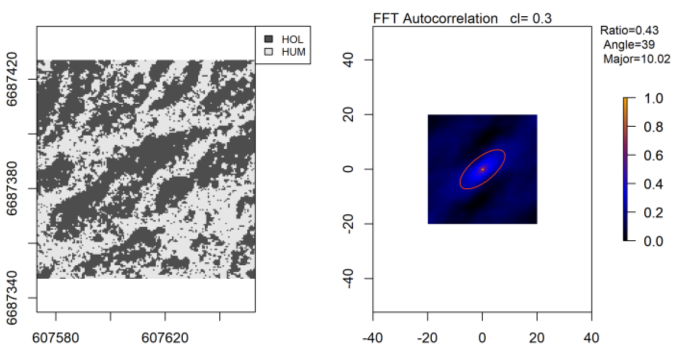

Figure 4.6. *An example of FFT output graph. It shows the patterning of hummocks (HUM-hummock) in a corner of Peatland 40 (on the southeast of Sweden, right next to an unnamed lake) on the left. HOL refers to any other classes. On the right, it is the graph of generalized overall patterning of hummocks in this buffer.*

Selection of suitable pattern metrics

Only hummock patches were chosen for analyzing patch characteristics. It was realized with the software of Fragstats (reference). In total, there were 38 pattern metrics generated. Among these metrics, MEAN (Mean patch area) and GYRATE (Radius of gyration) were both highly related to the area of land-cover types. Besides, the latter one also reviled the shape of land-cover patches. PLAND (Percentage of landscape) had no direct connect to either patch area or shaping (in the class level), but provided component proportion ratio between hummock patches and the land-cover entity in designated peatlands. The detailed information of the adopted pattern metrics can be found in Table 4.2.

Table 4.2. *The selected pattern metrics for analyzing the correlation to climatic development along gradients.*

Number	Metric	Description	Category (according to functions)		
			Area	Shape	Land cover Composition
1	AREA_MN (Mean patch area)	AREA stands for Patch Area Distribution; this metric is based on the class level and explained by distribution statistics (mean)	√		
2	GYRATE_MN (Radius of gyration)	GYRATE stands for Radius of Gyration Distribution; when aggregated at the class level, it provides a measure of landscape connectivity (correlation length); With values of other factors the same, it is bigger with the increment of patch size; if holding area constant, the more extensive the hummock patch (elongated and less compact), the greater the metric of Radius of Gyration	√	√	
3	PLAND (Percentage of landscape)	PLAND represents the percentage the selected peatland comprised of the corresponding land cover type (hummock, in this study); it is a relative measure, it is rather a measure of landscape (peatland) composition than class area for comparing between peatlands of different sizes; range: (0,100]			√

5 | Results

5.1 Land-cover Classification

This section will mainly discuss about the quality of land-cover classification by groups (defined in Table 4.1). The classification result of the 2nd round classification will be emphasized. As for classification accuracy, it will be compared by (statistical) classification accuracy assessment and visual check criteria.

5.1.1 Overall classification result

Classification accuracy assessment was only conducted in the representative peatlands. The lower limit of acceptable classification accuracy was set to 70%. As can be seen in Table 5.1, the average overall classification accuracy of representative peatlands is 66.67%, less than 70%. In the 2nd round classification (Table 5.2), it significantly improved to 84.35%, with almost excellent level of agreement (Table 5.2 and Table 5.3), which means the final classification result is totally acceptable. Among classes, water and forest were classified well, while MLC algorithm frequently got confused with classifying mud-bottom.

As for other peatlands (except from representative peatlands), their overall classification accuracy was relatively inferior to that of representative peatlands, according to the visual check. Salt-and-pepper effect arose when the MLC algorithm got confused between possible land-cover types when identifying pixels. Apart from that, the visual assessment indicated some general problems occurred during classification process for those peatlands: 1) some big patches of hummocks around forests were classified to be larger than reality (Figure 5.1(d)); 2) for areas with dense striping hummocks, the amount and total area of hummock patches were less than the ground truth (Figure B.2). The above-mentioned points restricted the average classification accuracy of approximately 5% to 15%.

Table 5.1. *An overview of classification accuracy assessment result (1st round classification, with RGB input, 10-meter radius buffer).*

Peatland Location number	Overall accuracy	Kappa Index	User's Accuracy					Producer's Accuracy				
			Classes					Classes				
			Hummock	Hollow	Water	Forest	Mud-bottom	Hummock	Hollow	Water	Forest	Mud-bottom
18	0.7143	0.6228	0.67	0.83	1.00	1.00	0.25	0.57	0.63	1.00	1.00	1.00
14	0.7143	0.6261	0.83	0.83	1.00	0.33	0.50	0.71	0.83	1.00	0.50	0.50
27	0.7143	0.6205	0.83	0.83	1.00	1.00	0.00	0.63	0.63	1.00	1.00	0.00
5	0.6667	0.5559	0.83	0.67	0.50	0.67	0.50	0.63	0.57	1.00	1.00	0.67
2	0.6190	0.5030	0.83	0.67	0.00	1.00	0.25	0.63	0.80	0.00	0.43	1.00
34&35	0.5714	0.4408	0.67	0.50	0.00	1.00	0.50	0.50	0.75	0.00	0.60	0.50
Average	**0.6667**	**0.5615**	0.78	0.72	0.58	0.83	0.33	0.61	0.70	0.67	0.75	0.61

Table 5.2. *Accuracy assessment result of the 2nd round classification, with RGB/IR/DEM input, 1-meter radius buffer.*

Peatland Location	Overall accuracy	Kappa Index	User's Accuracy					Producer's Accuracy				
			Classes					Classes				
			Hummock	Hollow	Water	Forest	Mud-bottom	Hummock	Hollow	Water	Forest	Mud-bottom
18	0.9524	0.9382	1.00	0.83	1.00	1.00	1.00	0.86	1.00	1.00	1.00	1.00
14	0.8571	0.8142	1.00	0.83	1.00	1.00	0.50	0.75	1.00	1.00	0.75	1.00
27	0.7619	0.6912	0.83	0.83	1.00	1.00	0.25	0.71	0.83	1.00	0.60	1.00
5	0.8571	0.8136	1.00	0.67	1.00	1.00	0.75	0.75	0.80	1.00	1.00	1.00
2	0.7619	0.6930	0.83	0.67	1.00	1.00	0.50	0.83	0.67	1.00	0.60	1.00
34	0.8571	0.8184	0.83	1.00	1.00	1.00	0.50	1.00	1.00	0.50	0.75	1.00
35	0.8571	0.8169	0.83	0.83	1.00	1.00	0.75	1.00	1.00	1.00	0.60	1.00
Average	**0.8435**	**0.7979**	0.90	0.81	1.00	1.00	0.61	0.84	0.90	0.93	0.76	1.00

Table 5.3. *An Interpretation of the agreement between the independent examiners according to Kappa Coefficient (Souza, Azulay-Abulafia et al. 2011, McHugh 2012).*

Value of Kappa coefficient	Level of agreement
0	Absent/None
(0,20]	Minimal
(20,40]	Weak
(40,60]	Moderate
(60,80]	Good/Strong
(80,100]	Excellent

5.1.2 Classification results by groups

The interpretation of classification results (by groups) will not be elaborated to every peatland, but emphasized on the representative peatlands. For other peatlands, their classification results will be summarized with visual assessment by groups. The discussion in this section is closely related to a large number of graphs. Firstly, classification results of all of the representative peatlands and examples of other peatlands are provided (Figure 5.1 and Appendix B). For assessing classification accuracy, Table 5.1 and Table 5.2 are referred to. Secondly, the visual check (Figure 5.2 and Appendix C) is frequently referred to. It consists of the criteria of salt-and-pepper effect, average patch size of hummocks and striping patterning of hummock patches. Besides, the distribution of hummocks, together with original RGB images, is also shown in the same graph.

Group 1 (Very Low temperature)

In this group, Peatland 18 (63.284°N, 12.422°E, located on the east of Scandinavian Mountains) was selected as the representative peatland. Results of land cover classification and original RGB image of example areas in this peatland are shown in Figure B.1. Hummocks showed striping patterns in the northern and central part of the peatland. The borders between land cover types were not hard to distinguish in this peatland. Accordingly, the user's accuracy and the producer's accuracy of hummock were both high enough, with 100% and 85.71% respectively. The overall classification accuracy was also increasing from 71.43% (of 1st round classification) to 95.24% (2nd round). Kappa coefficient reached the value of 0.9382, which means that the level of agreement was almost perfect. (Table 5.1 and Table 5.2)

As shown in Figure C.1, robustness of the method of MLC in this group was moderate, judged by the rather significant rating value of salt-and-pepper effect (group average: 3.4). Patch size of hummocks in most sites were relatively small, except of peatland 45 (66.500°N, 21.717°E, on the far north of Sweden) and peatland 46 (67.298°N, 20.812°E, also on the far north, close to peatland 45 on its west). Hummocks in all of peatlands did not show much striping patterning. The RGB images of peatlands in location 32 and 46 presented in yellowish hue, while others showed in greenish hue (see left column in Figure C.1). MLC performed badly, as hummocks and hollows misclassified into each other in central areas. Classified map of peatland 45 is shown in Figure 5.1(a). Several speckles, resulted from salt-and-pepper effect, can be seen in the lower right corner.

Group 2 (Low temperature)

Peatland 14 (62.248°N, 14.453°E, in the central area) was chosen as the representative peatland in this group. Hummocks in this peatland showed highly striping patterning, which were extracted well in the classification (Figure B.2). The general quality of both rounds of classification was acceptable. However, they both did not perform well in the bottom-left area. The actual hummock size should be in between the classification results. The user's accuracy of hummock was higher than its producer's accuracy, with 100% and 75% respectively (Table 5.2). Approximately three fourths of hummocks were correctly shown on the classified map. The overall classification accuracy improved from 71.43% to 85.71%. Kappa coefficient exceeded 0.8 (reaching 0.8142), which means that the level of agreement was strong (Table 5.3).

According to visual assessment (Figure 5.2(a)), the salt-and-pepper effect is to the same extent as group 1. Over half of peatlands in this group have rating of equal or greater than 4. But, the signature file still works well in two "neighboring" peatlands of Peatland 14, which are Peatland 13 and Peatland 15. These three peatlands were all located in the center of Sweden, lined up and close to each other (< 100km). The great performance was possibly due to: 1) vegetation patterning in Peatland 14 was critically heterogenous, providing a diversity of signature profiles in training samples; 2) peatlands consist of similar vegetation in short spatial distance. The average patch size is considerable, with rating of 3.7.

Figure 5.1. *Examples of land-cover classification results of peatlands. The figure consists of a series of graphs, which are named with alphabets from a. For each subgraph, the classified maps of the 1st round classification (RGB image input, 10m-radius buffer surrounding sample points), the 2nd round classification (RGB, IR images and DEM input, 1m-radius buffer surrounding sample points) and original aerial images (RGB band) are shown from left to right.*

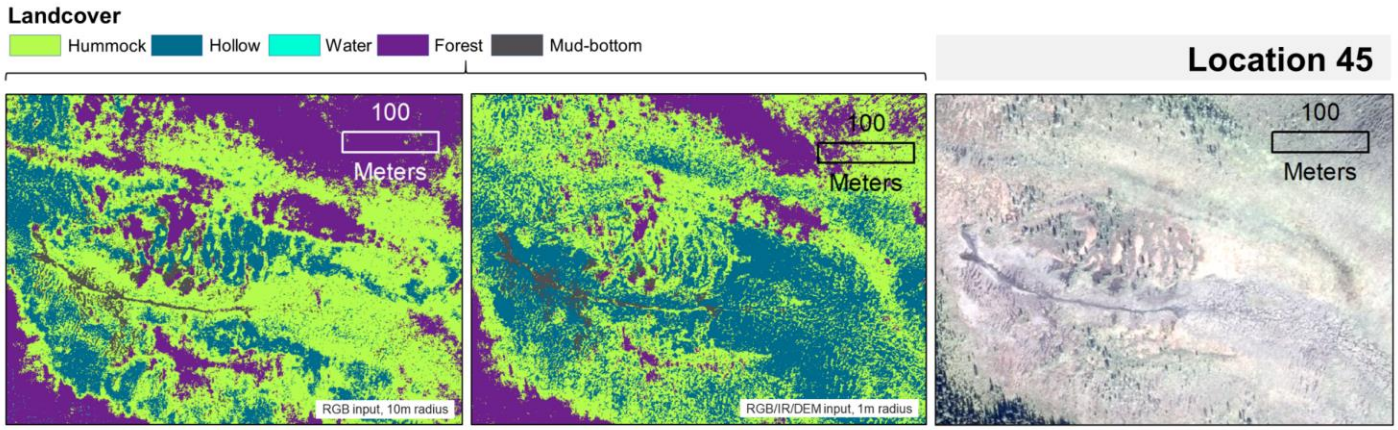

(a) An example of "normal" peatlands (where signature files applied to) —— Peatland 45 (66.500°N, 21.717°E, located on the far north of Sweden, near Suobbat) in Group 1(group with very low temperature)

Peatlands with highly striping hummocks take up almost half of the total.

Group 3 (Moderate temperature)

As for peatland location 27 (the representative peatland in group 3; 60.899°N, 16.075°E, on the mid-south of Sweden), several ponds in the central area were surrounded by layers of striping hummocks (Figure 5.1(b)). These hummocks were wrongly classified as mud-bottoms in the 1st-round classification. The user's accuracy of hummock was higher than producer's accuracy (83%/71%). The overall accuracy improved slightly from 71.43% to 76.19%. Compared to representative peatlands in other group, this result was not satisfying. Kappa coefficient was 0.6912, indicating that the level of agreement was moderate.

As can be seen from Figure 5.2(b), there is no significant salt-and-pepper effect in the classified maps except Peatland 9, which indicates that the robustness of MLC in this group is great. Average patch size of hummocks is moderate. Highly-striping hummocks are distributed in the peatland locations of 25 (60.165°N, 14.718°E, on the mid-south of Sweden, close to the border between Örebro and Dalarna), 27 and 40. Amazing hummock-hollow vegetation patterning was witnessed in peatland location 40, as shown in the second picture of Figure 5.1(c). Long and thin hummock stripes spread out in circles, which looks like a huge spider web. Besides, the overall classification accuracy of Peatland 10 (58.063°N, 13.199°E, on the south-west) was relatively low by visual check, since densely-covered mud-bottoms with tiny hummock patches surrounde-

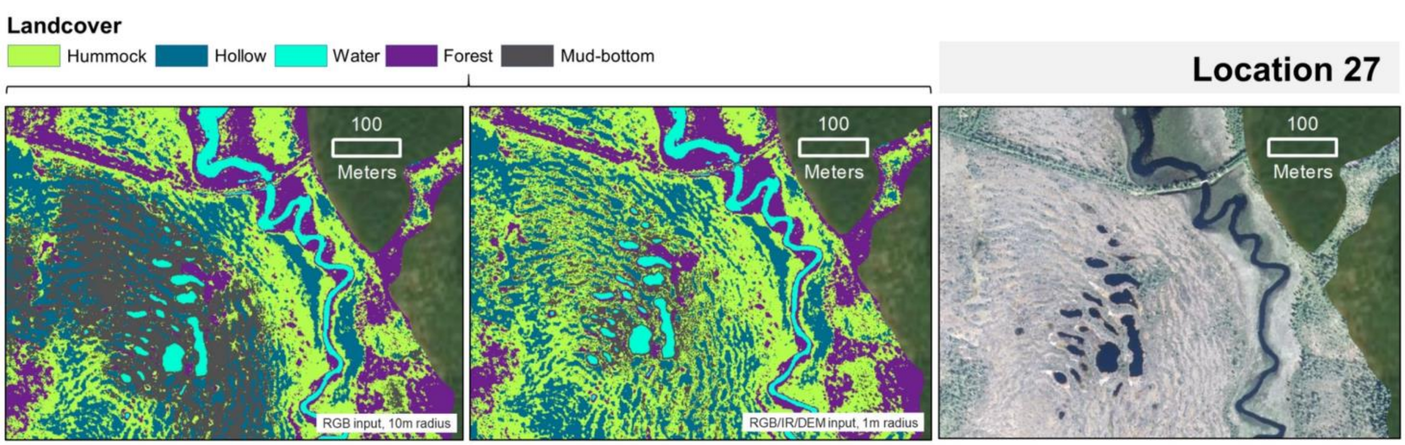

(b) The representative peatland —— Peatland 27 (60.899°N, 16.075°E, located in the middle of Sweden, not far from the lake of Hyn) in Group 3 (group with moderate temperature)

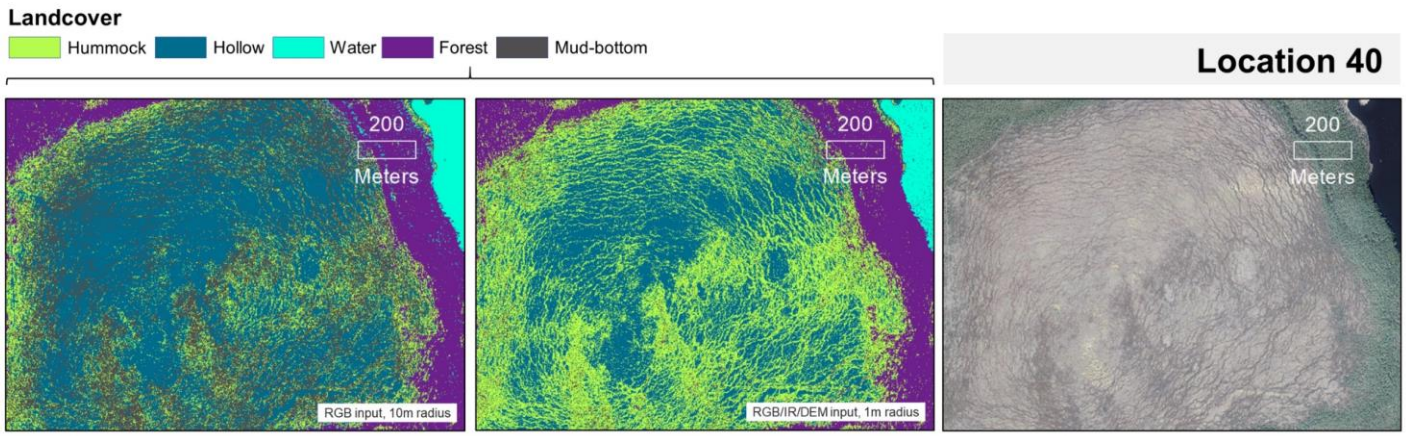

(c) An example of other peatlands —— Peatland 40 (60.311°N, 16.939°E, on the southeast of Sweden, close to Uppsala and Stockholm) in Group 3 (group with moderate temperature)

-d in the central area suppressed the accuracy of MLC algorithm.

Group 4 (High temperature)

The representative peatland in group 4 (Peatland 5, 57.496°N, 14.249°E, on the south of Sweden) had striping hummocks roughly from northwest to southeast and intertwined with mud-bottom stripes. The user's accuracy of hummock was excellent (100%). However, it did not actually mean that all of hummocks were correctly classified, since the amount of validation points was not great enough. The user's accuracy would have been highly possible to become lower if more validation points were put in research area. Surprisingly, the overall classification accuracy achieved an increment from 66.67% to 85.71%. The level of agreement was strong, judged by high kappa coefficient (0.8136). The classification result of Peatland 6 (an example of peatlands in group 4) is shown in Figure B.5.

Noticeable salt-and-pepper effect is observed in Peatland 6 (57.317°N, 14.269°E, in Jonkoping County, on the south of Sweden) and Peatland 7 (58.080°N, 12.734°E, in Västra Götaland County, on the south-west) (Figure C.2). The rest of peatlands have the value of either 2 or 3, which means that it shows good robustness. Most of peatlands in this group had medium size of hummock patches. The majority of peatlands did not show striping patterning of hummocks. Only Peatland 36 (58.434°N, 13.785°E, next to Skövde city, on the south of Sweden) showed greatly striped hummocks widespread.

Group 5 (Very high temperature)

As mentioned in Section 4.2.3, the selection strategy of representative peatlands helped improving classification accuracy of peatlands, where signature files applied to, significantly.

For representative peatlands themselves, the performance of MLC also improved greatly from round to round. As for Peatland 34 and Peatland 35, the overall classification accuracy increased from 57.14% (of the entity) to 85.71% for both (Table 5.1 and Table 5.2). What's more, salt-and-pepper effect were mostly eliminated. Striping hummocks showed up in classified images. Kappa coefficient has increased drastically from 0.4408 to 0.8184 and 0.8169 for Peatland 34 and Peatland 35, respectively. The level of agreement reached the excellent level for both. Besides, the overall classification accuracy of Peatland 2 rose from 61.90% to 76.19% (Table 5.1 and Table 5.2). The level of agreement was good. The classification result of Peatland 20 (example of peatlands, other than the representative peatland, in group 5) is shown in Figure B.3.

As shown in Figure C.3, many salt-and-pepper patches are found in Peatland 3 (56.782°N, 14.069°E), Peatland 4 (56.833°N, 14.094°E), Peatland 19 (56.313°N, 13.506°E) and Peatland 20 (56.269°N, 13.553°E). The average rating of salt-and-pepper effect is relatively high in this group (3.3). Average patch size of hummocks is moderate. Hummocks are to some extent bigger in Peatland 19 and Peatland 34. Different from other groups, no peatland in this group shows highly striping patterning of hummocks, with the average rating of merely 1.7.

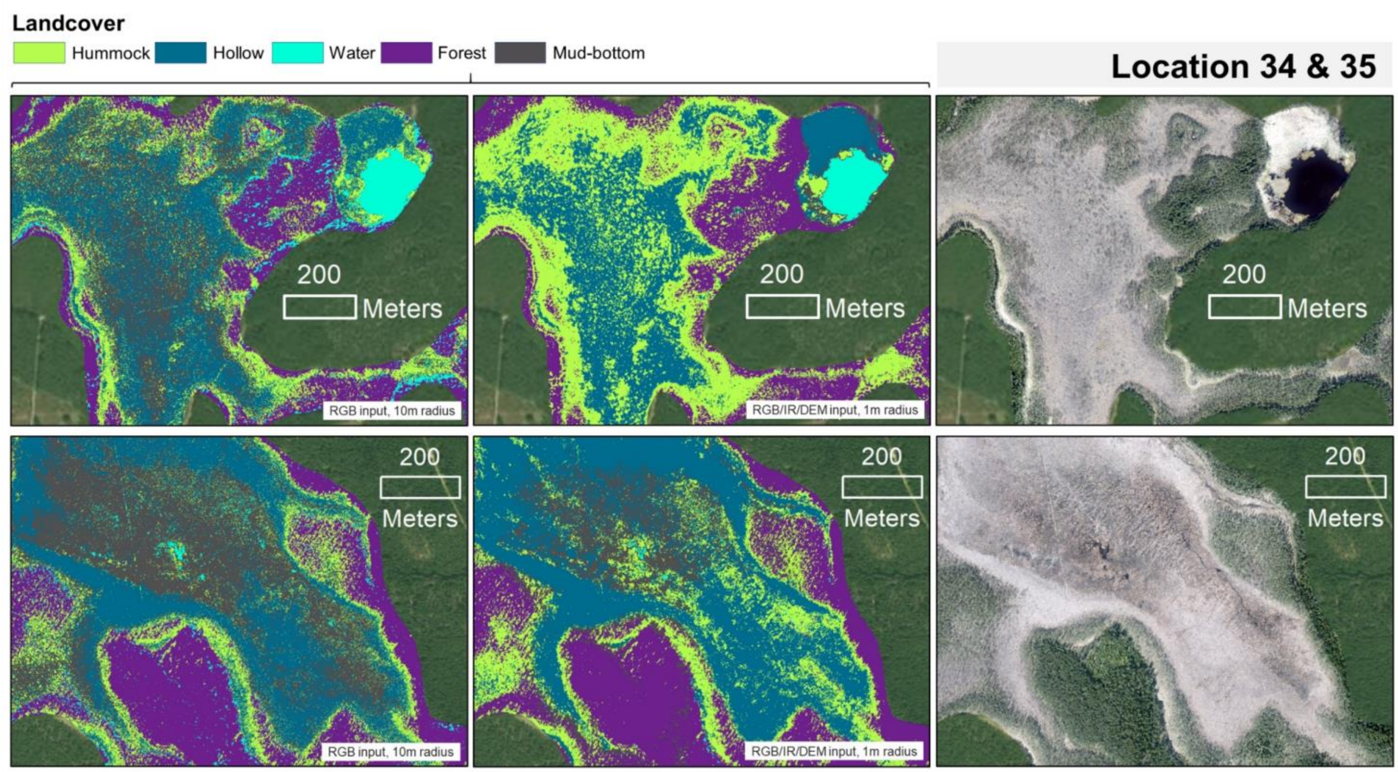

(d) The representative peatlands —— Peatland 34 and Peatland 35 (both at 56.823°N, 15.278°E, on the southeast of Sweden) in Group 5 (group with very high temperature)

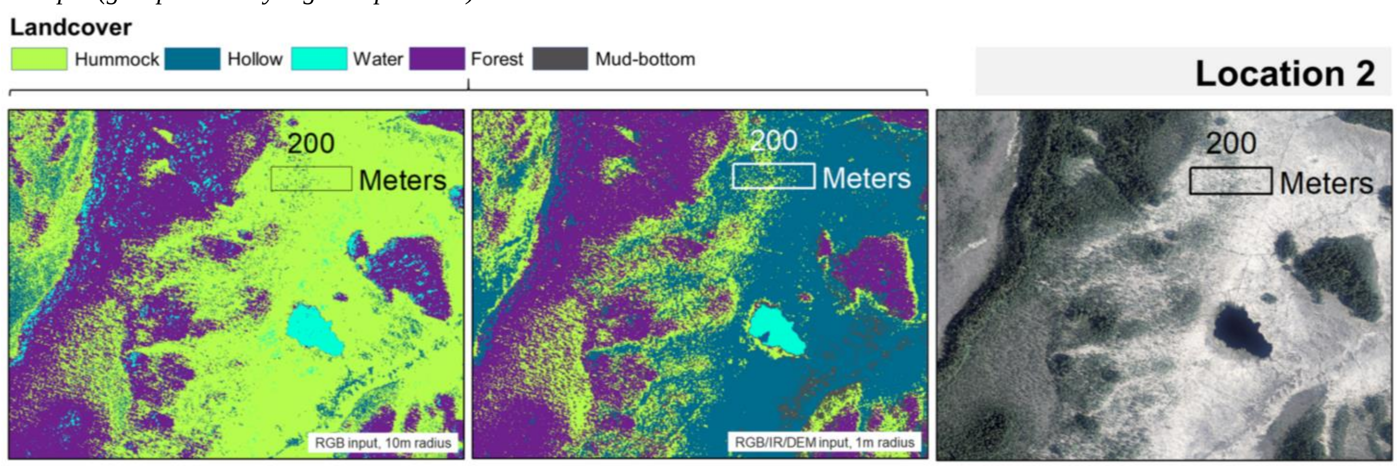

(e) Another representative peatland —— Peatland 2 (56.802°N, 13.522°E, on the southwest, not far from the lake of Torserydssjön) in Group 5 (group with very high temperature)

5.1.3 An overview of visual assessment results (inter-groups)

Visual assessment was used as a supplementary means of interpreting classification results. Visual assessment results of 5 groups are shown in Figure 5.2 and Appendix C. As can be seen in Figure 5.3, Salt-and-pepper effect is more remarkable in Group 1, Group 2 and Group 5. It indicates that the robustness of MLC in Group 3 and Group 4 is stronger than other groups. In other words, the performance of signature files' being applied (to normal peatlands) in Group 3 and Group 4 are better. Speaking to the average patch size of hummocks, the high score is witnessed in Group 2, much higher than other groups. However, the patch size of hummocks has still trended down from cold regions to warm regions (Group 1 to Group 5). Likewise, it is also highly striping of hummocks in Group 2. Striping Patterning follows a declining curve from north to south (of Sweden), too. So, the patches of hummocks on the south are less striping (elongated) than that on

Figure 5.2. *Visual assessment results by groups. From left to right in the graphs: peatland number, aerial images of peatlands (in RGB band), hummocks' distribution extracted from classified maps, visual assessment criteria (1) Salt-and-pepper effect in maps of hummocks' distribution, 2) Average patch size of hummocks, 3) (The extent of) striping patterning of hummocks). They are rated form the number of 1 to 5, the legend is shown on the right.*

(a) Visual assessment result of Group 2 (group under low-temperature condition)

Peatland number	Aerial imagery (RGB)	Classified map (2nd round)	Visual assessment criteria (1-5 rating)		
			Salt-and-pepper effect	Patch size (Hummock)	Striping (Hummock)
13	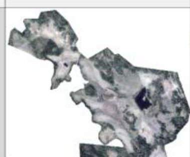	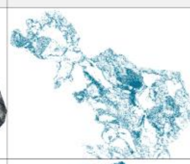	3	3	3
14	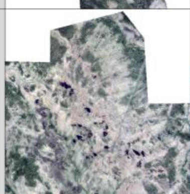	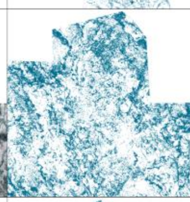	2	4	5
15			1	4	4
29		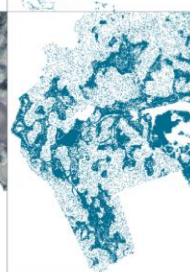	5	4	2
30		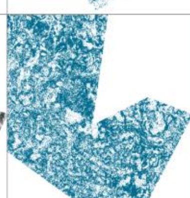	4	5	3
42		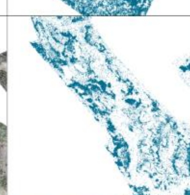	4	3	4
44			4	3	2
Average			**3.3**	**3.7**	**3.3**

Description

Salt-and-pepper effect

1 Only found in very a few regions

2 Found in a few regions

3 Easily found in some regions (without zooming in very much)

4 Spread over the map

5 Spread all over the map and very easily recognized without zooming in

Patch size of Hummock

1 Very small

2 Small

3 Moderate

4 Large

5 Very large

Striping pattering of Hummock

1 No / Very a few stripes found

2 A few stripes found

3 Several stripes found, distributed as clusters in the map

4 Many stripes found, distributed all over the map

5 Highly-striping

(b) Visual assessment result of Group 3 (group under moderate-temperature condition)

Peatland number	Aerial imagery (RGB)	Classified map (2nd round)	Visual assessment criteria (1-5 rating)		
			Salt-and-pepper effect	Patch size (Hummock)	Striping
9		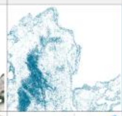	4	2	2
10		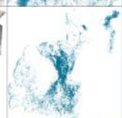	2	2	2
12		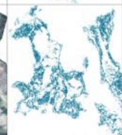	1	3	2
25		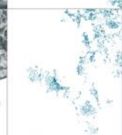	2	2	4
26		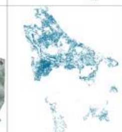	2	2	2
27			1	4	4
39			2	3	3
40	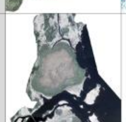		3	3	5
41			2	3	2
Average			**2.1**	**2.7**	**2.9**

the north. More accurate results of peatland vegetation patterning will be shown in the following section, where a series of pattern metrics are plotted with climatic variables.

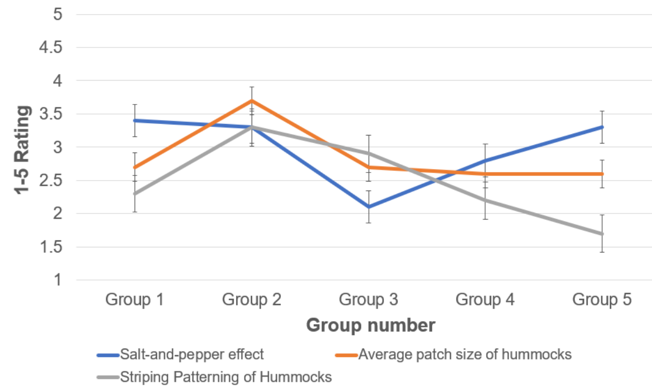

Figure 5.3. *Comparison of visual assessment criteria (values) among groups (the vertical lines with end-lines are error bars)*

5.2 Pattern analysis

5.2.1 Correlation between the pattern metrics and climatic variables

As for the correlation between a series of pattern metrics and climatic variables, the tendency was not greatly significant. Large variation of pattern-metric values under similar climatic conditions was witnessed. Besides, R^2 (coefficient of determination) value was low of most of correlations (displayed in Figure 5.4 and Appendix E). It indicated that the linear models (prediction) explained not much of the variety of the pattern-metric values (response data in this case) around its mean.

Among all of the correlations to temperature, Anisotropy-temperature correlation had the highest R^2 value of 0.18 and only it showed an upward trend in from cold region to warm region. All of other correlations showed downward trend from north to south of Sweden, from cold to warm areas. R^2 values were in between 0.11 to 0.12, except Percentage of Landscape - temperature correlation (with merely 0.04). Similarly, all correlations to precipitation except Anisotropy - precipitation correlation characterized decreasing trend of metric values from humid regions to relatively dry regions. R^2 values were greater in Radius of Gyration (Mean) - precipitation correlation and Percentage of Landscape - precipitation correlation, with 0.11 and 0.10 respectively. Other correlations were featured with R^2 values lower than 0.10, from 0.03 to 0.07.

From every sub-graph in Figure 5.4 and Figure E.1, a great many points outside confidence interval can be seen. These values significantly deviate from regression line. For metrics of Major, Minor and

Anisotropy (with temperature on x-axis), the deviated points have similar distribution characteristics in scatterplots. The distribution of points in scatterplots of Radius of Gyration and Percentage of Landscape do not follow the same rule. For pattern metrics - precipitation correlations, Major-P and Minor-P have similar distribution of points. Point's distribution in Aniso-P is not close to the above-mentioned two. GYRATE_MN-P and PLAND-P have even more chaotic distribution of points. Average values of pattern metrics in all peatlands can be checked by Table E.1. Density curves of pattern metrics (on the right of scatterplots) are plotted for exploring "stable states". Curves in all graphs have shown double peaks. Moreover, upper peaks are always less steep than lower peaks. "Troughs" in between are shallow.

Figure 5.4. *Scatterplot with density curves, showing the correlation between specific pattern metrics and climatic variables. Regression line and 95% confidence interval are also shown in graphs. Colors of points are classified by groups.*

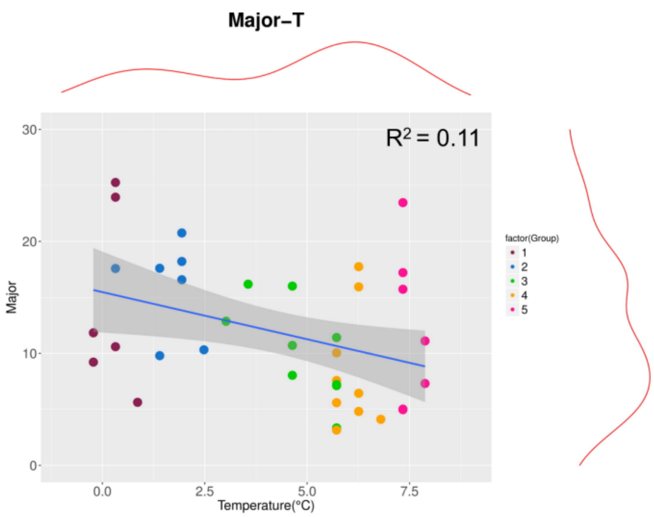

(a) The correlation between the pattern metric of Major and climatic variable of temperature

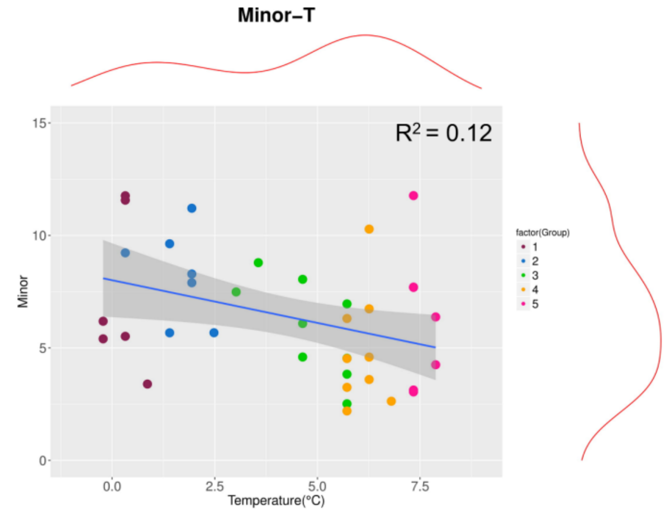

(b) The correlation between the pattern metric of Minor and climatic variable of temperature

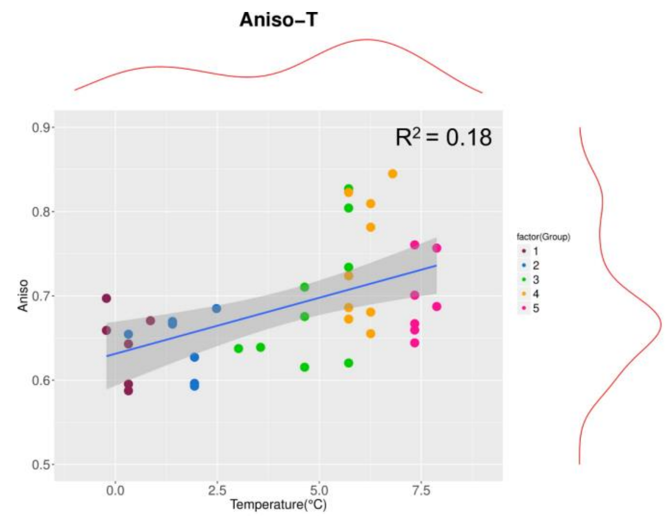

(c) The correlation between the pattern metric of Anisotropy and climatic variable of temperature

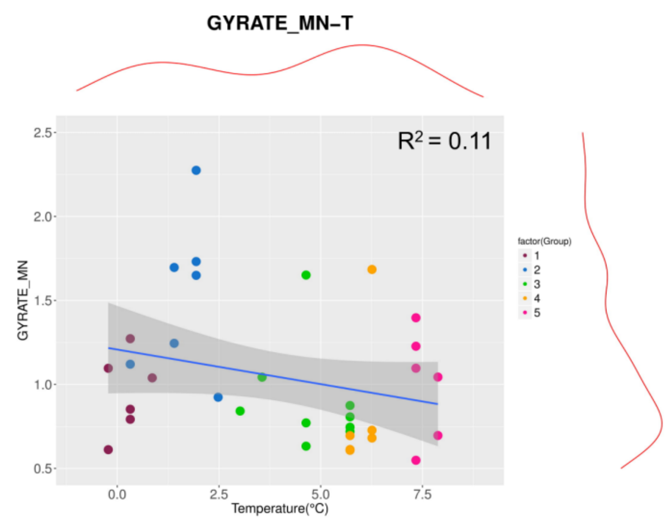

(d) The correlation between the pattern metric of Radius of Gyration-Mean and climatic variable of temperature

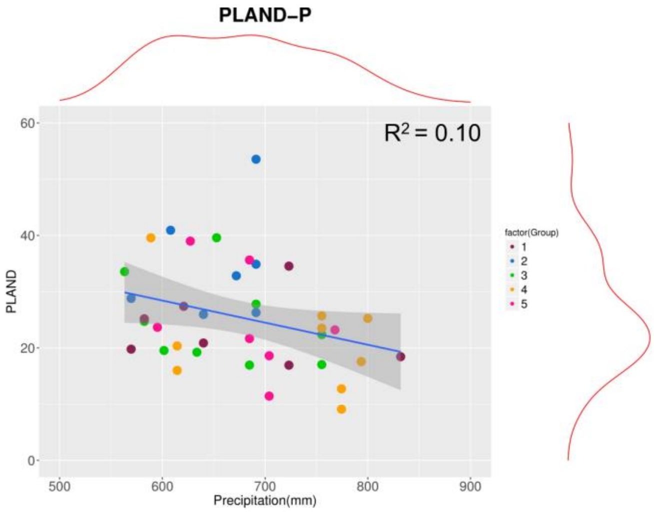

(e) The correlation between the pattern metric of Percentage of Landscape and climatic variable of precipitation.

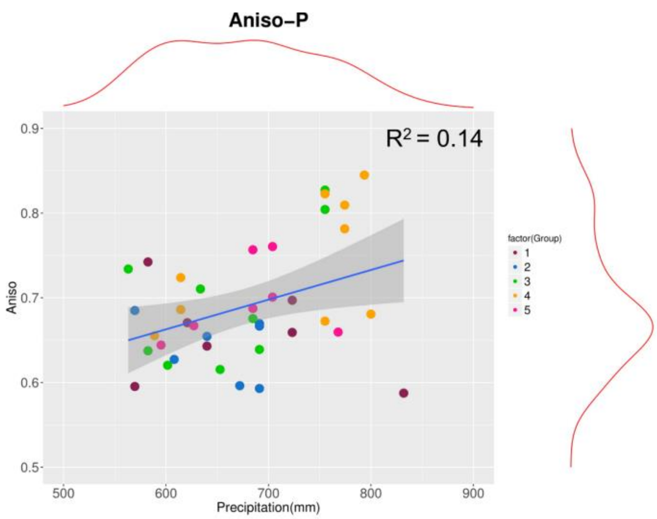

(f) The correlation between the pattern metric of Anisotropy and climatic variable of precipitation.

5.2.2 Relation between the pattern metrics and Sub-areas

Sub-areas were divided according to climatic variables of temperature and precipitation. It is also feasible to replace accurate temperature or precipitation values with pre-defined sub-areas for examining relations between peatland vegetation patterning and climate development. For instance, boxplot of Major-temperature sub-areas (Figure 5.5(a)) illustrates variation of Major values between groups. The highest mean value is found in Group 2 (Temperature sub-region 2), while the lowest is of Group 4. A downward trend from Group1 (the coldest region) to Group 5 (the warmest region) is exhibited, which corresponds to the trend in Figure 5.4 (a). Focusing on the grey bars, which show 90% confidence interval of mean metric values, we can see that there is a jump from Group 2 to Group 3. The transition here is greatly more significant than other "neighborhoods". From Group 4 to Group 5, an increment is witnessed again.

***Figure 5.5.** Boxplots depicting the relation between Major and temperature sub-areas (groups used for preparing signature files) or precipitation sub-areas. Other important elements are also shown in the plot: 1) Sample means – plus signs, 2) 90% confidence interval of means – grey bars in the middle of boxes, 3) Data points (of Major) - Jittered points in red.*

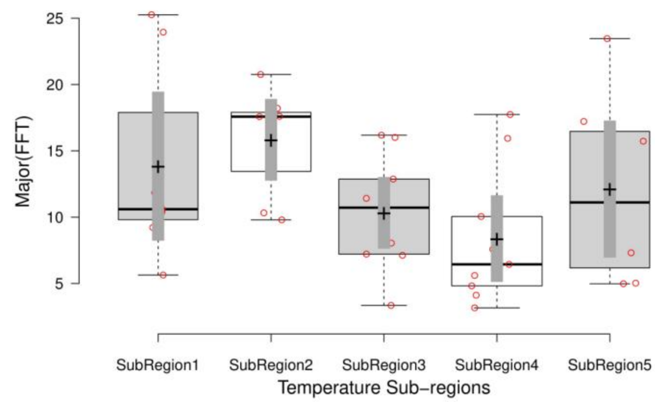

(a) Major – Temperature sub-areas

Boxplot of Major-precipitation sub-areas (Figure 5.5(b)) depicts variation of Major values between groups. The trend is not apparent, since there are not enough precipitation sub-areas. After declining slightly from Precipitation Sub-area 1 to Precipitation Sub-area 2, an increment to some extent is shown between Sub-area 2 and Sub-area 3.

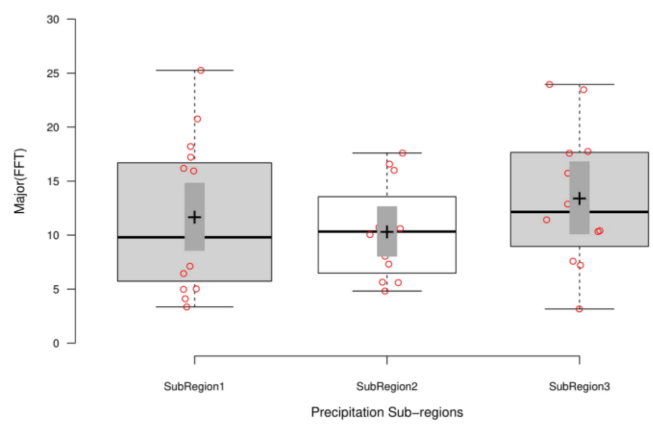

(b) Major – Precipitation sub-areas

In the end of this chapter (next page), several examples of hummock-hollow microform in sample peatland are shown with identifying locations. It correspond to the previous results in sections 5.1.2 and 5.1.3 to some extent.

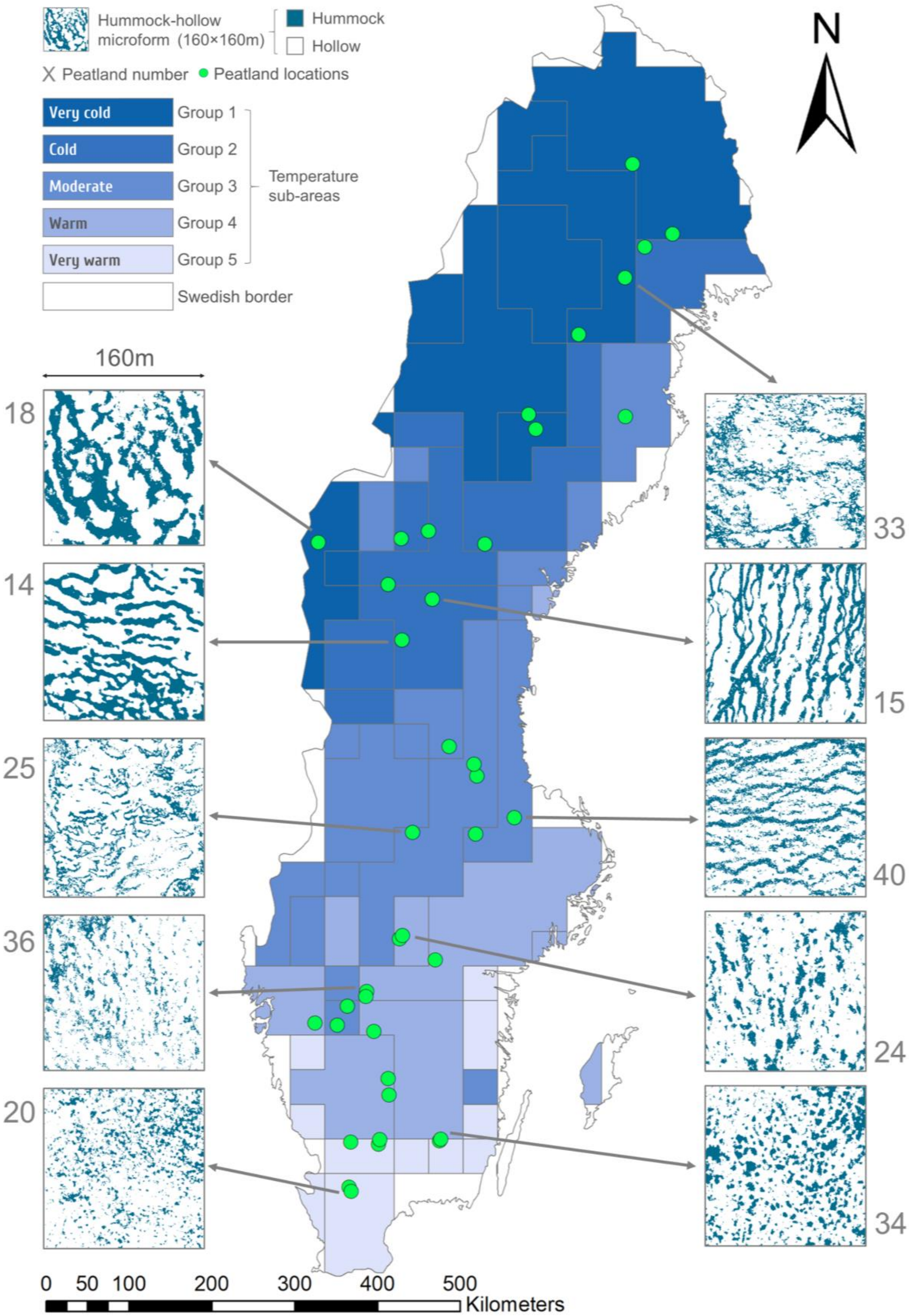

Figure 5.6. *An overview of 5 climatic groups (classified according to annual average temperature) and representative examples of hummock-hollow microform in selected peatland locations from cold region to warm region in Sweden. 2 peatlands in each group are chosen. The tiles are all with the size of 160×160m. Those are all located in the central area of peatlands (where hummock-hollow microtopography are easily to observed).*

6 | Discussion and Recommendation

This study researched the use of high-resolution aerial imagery in analysing peatland vegetation patterning along climatic gradients. Overall speaking, the patterning of hummock-hollow microform was well-detectable. Vegetation patterning characteristics were mostly preserved well.

6.1 Discussion

6.1.1 The overall accuracy and robustness of the used classification method

The large scale of the research area brought about great variability of vegetation characteristics in peatlands. Dominant vegetation differed between mire regions (Figure 3.2). Taking the above-mentioned into consideration, it was hard to apply much detailed classification key to classification of peatlands. One feature peatlands showed in common was that peatland vegetation formed hummock-hollow microform, regardless of species composition of peatland vegetation. In addition, hummock-hollow microform was the most detectable patterning characteristics from aerial view. Thus, we only used hummock-hollow microform to refer to peatland vegetation patterning. Apart from this, mud-bottom was the most distinguishable land-cover type in all mire regions. In the ordered images, forest and water were also distributed widely. Together with above-mentioned classes, those land-cover types can be easily found in images. To summarize, proper number of classes and simplified microform had a positive impact on overall classification accuracy.

This study reached a high overall classification accuracy of 84.35% with Kappa index of 0.80 for representative peatlands. Prior researches on peatlands in other countries also showed acceptable overall classification accuracy with MLC. As it goes to tropical regions, Wijaya, Reddy Marpu et al. (2010) used TerraSAR-X data for characterizing peatlands in tropical swamp forests of Indonesia. The overall classification accuracy reached 87% with Kappa Index of 0.85. Moving to northern Europe, Holopainen and Jauhiainen (1999) detected changes in peatland vegetation of southern Finland by comparing aerial images from different years. The overall accuracy of 66.5% and 55.6% corresponded to newer images and older images respectively. In Canada, where it has one of the largest areas of peatlands, Racine, Bernier et al. (2005) used 4 classes or 10 classes for classifying several peatlands in Quebec. Textures generated from multitemporal images were used for MLC. Those multitemporal images had fine-mode and standard-mode images. Their results showed that overall accuracy using 4 classes (fine-mode: 37%, standard-mode: 74%) was higher than using 10 classes (fine-mode: 35%, standard-mode: 59%).

Representative peatland locations, which were selected for preparing the signature files, determined the quality of classification results in this study (Figure 5.2). Ideally, if peatlands with similar spectral signature of all classes are in the same group, sharing one signature file from this group, then the robustness of will be great. However, it was unlikely to happen in real cases. In this study, peatlands were divided into groups according to temperature difference and it showed acceptable robustness with this method (Figure 5.2 and Figure 5.3). Salt-and-pepper effect was moderate on average. Actually, we also tested applying a signature file, which contained spectral signature of land-cover classes from all peatland locations in the same group (Group 4), to peatlands in another group (Group 5). It showed better performance in robustness. Overall classification accuracy improved greatly by visual check.

6.1.2 Peatland vegetation patterning along temperature gradient

It was hypothesized that the average patch size of hummocks is going to show uptrend from cold regions to warm regions (generally follows the latitudinal gradient). A series of prior studies by ecologists have revealed the effect of temperature on competition between hummock and hollow (Breeuwer, Heijmans et al. 2008, Eppinga, Rietkerk et al. 2008, Kleinen, Brovkin et al. 2012). Breeuwer, Heijmans et al. (2008) found that biomass production of all Sphagnum (one hummock-forming species) species increased with the increment in temperature. Nutrient concentrations around hummocks were becoming higher, thus, hummocks gradually dominated the hummock-hollow microform and hollows lost competitive strength in warm regions, leading to bigger area of hummock.

The results of this study showed that hummock followed an overall downtrend in size and a higher anisotropy tendency with the increment of temperature, predicted by linear regression model (pattern metrics ~ temperature) (Figure 5.4 and Appendix E). But, the correlation was not significant. As for values of all of the selected pattern metrics, their distribution was with a wide range under similar temperature conditions. We acquired more information from the boxplots, which depicted relations between pattern metrics and sub-areas (Figure 5.5). If we turn to Figure 5.5 (a), Major is now used for representing average patch size of hummocks (Major × Minor refers to average area; Minor also follows the same trend in Appendix E). Being located in the far north of Sweden, average patch size of hummocks in Group 1 is relatively smaller than hummocks in Group 2 (in the north-central region of Sweden). This result matches that observed in the study by Rydin, Sjörs et al. (1999). It says that the hummock-hollow microform is mostly found inside relatively large bogs in central regions of Sweden. While, ombrotrophic (meaning 'rain-fed') locations are more likely to be found, where their hollows are poorly grown. Sphagnum growth is also lagged behind. Accordingly, hummocks are generally smaller than that of its neighboring southern regions.

6.1.3 Peatland vegetation patterning along precipitation gradient

Lindsay, Rigall et al. (1985) researched on the influence of rainy days within a year on hummock-hollow microforms in British peatlands. This paper showed a map in the similar layout to Figure 5.6. According to that map, the number of rainy days during one year reduces from north to south. Hummock size increases with lesser rainy days. However, the findings of the current study do not support the above-mentioned research by Lindsay, Rigall et al. (1985). In this study, I chose annual precipitation as climatic variable, instead of using rainy days per year. As can be seen in Figure 5.4 and Appendix E, more precipitation contributes to smaller patch size of hummocks. Actually, this result is consistent with one commonly accepted hypothesis which tries to explain the interaction between hummock and hollow in bogs. It holds the view that evapotranspiration in groundwater regime is the most important variable of influencing microform dynamics (Eppinga, Rietkerk et al. 2008). Drier conditions result in more (faster) evapotranspiration from groundwater, which is suitable for hummock-growing. Speaking of my study area, coastal regions to Gulf of Bothnia are not influenced by wind from North Sea and Norwegian Sea, thus, less precipitation is observed than western mountainous regions. Hummock is growing bigger under its drier climate.

6.1.4 Stable states of hummock-hollow microform

As a member of ecological communities, peatland is possible to give response to environmental changes in different ways (Kéfi, Holmgren et al. 2016). One possibility is responding in a smooth way to small and gradual changes in climate change; another would be staying in slow development until external conditions go through a threshold (at this point peatlands respond suddenly), abruptly switching to a new state, which can lead to losses or gains of species (Rietkerk, Ketner et al. 1996, Folke, Carpenter et al. 2010, Kéfi, Holmgren et al. 2016). In this study, much effort was put on figuring out at which point (in states or transition points) Swedish peatlands are now standing. We referred to spatial analysis instead of using time series analysis for getting insights of the impact of climatic development on peatland patterning in Sweden. It is possible that the latitudinal extent of Sweden is still not long enough for containing “tipping points” (or transitions) in peatland patterning. Thus, exact reasons behind the absence of apparent two stable states in pattern metrics in this study is unclear. It may be owing to the current state is not reaching transition points or has already passed over it. Follow-up studies can compare peatlands between countries, where it is rich in peatlands, sampling peatlands along climatic gradients for both.

This comparison may reduce the occasionality of selecting research area.

6.1.5 In need of high-resolution meteorological data input

In this study, the result of sub-area division illustrated mosaic-shaped boundaries. It was easy to find sub-areas consisted of separate fractions in different regions. Two factors resulted in it: 1) distribution of precipitation in Sweden did not fully follow the expected gradient (from Scandinavian Mountains to Gulf of Bothnia). Extremely high precipitation observations were gathering in mountainous areas deep in northwest and southwestern coastal regions (near Rössjön) (see Figure 3.1(right)); 2) difference in precipitation were disorganized by using low-resolution precipitation map. Besides, several selected peatlands were close to borders between sub-areas. Those peatlands would be classified to different sub-areas if we used meteorological map with higher spatial resolution. Moreover, the low resolution of meteorological data input also restrained sub-area division. Considering the relatively irregular rainfall distribution shown in map, dividing more sub-areas according to low-quality data was not convincing.

Time series of meteorological data that we have used was from 1961 to 1990, while acquisition period of high-resolution imagery was from 2011 to 2017. Temporal match between remote sensing imagery and meteorological data is preferred in follow-up studies. As can be seen from Figure 6.1, annual average temperature has an uptrend from 1961 to 2010. Annual precipitation is fluctuating around 650 mm for the last 30 years (1980-2010), increasing from around 600 mm, which was maintained for over a century (Figure 6.1).

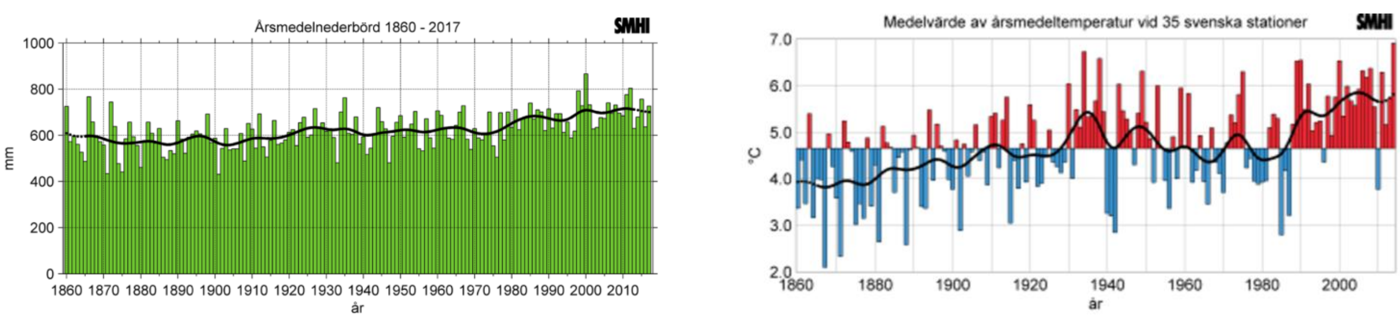

Figure 6.1. *Annual precipitation of Sweden from 1860 to 2017 (left) and annual average temperature of Sweden from 1860 to 2017 (right) (based on observation of 35 meteorological stations). (Source: SMHI)*

6.2 Recommendation

Except from the recommendation points, which were already discussed in the previous section, here I still here four points to present:

1) When analyzing impact of climate development on peatland vegetation patterning, other environmental variables should be held to constant. In this case, vegetation types in peatlands is actually a disturbing factor that has not been taken into consideration very much. Besides, interpreting aerial imagery visually for classifying peatland vegetation species was not enough. Spectral curve should be joined for helping to tell specific vegetation types in following studies.

2) I would propose to restrain mire regions for analyzing influence of climatic factors on peatland patterning in follow-up studies. Using each mire region (according to Gunnarsson and Löfroth (2009)) as one sub-region. Then, comparing value of pattern metrics along climatic gradients of each sub-region. Eventually, the influence of mire types (as a disturbing factor) will be also shown in results.

3) Sampling of suitable peatland locations was based on a map source with limited number of peatlands. Actually, Lantmateriet provides peatland distribution map with complete peatlands in Sweden, no matter how smll the size is. It also has a better overall quality regarding the accuracy of borders. The only problem is that it is too large in data size. The database shows zip files of peatland distribution maps in folders of counties of Sweden. Each county has over 600 MB data. Link to database (open data): ftp://download-opendata.lantmateriet.se/GSD-Terrangkartan_vektor/

4) There were no fieldwork data of ensuring ground truth in study locations. Thus, the result of classification accuracy assessment was not accurate. Ground truth points in several representative peatlands would be helpful for checking classification accuracy, if applicable in the follow-up studies.

7 | Conclusion

This study was trying to use remote sensing and pattern analysis for understanding the development of hummock-hollow microform along climatic gradients in Sweden. We were not confident of the feasibility of sampling peatlands in such a big scale (whole Sweden), even though there were hypotheses from other studies. Several pieces of conclusions from this study will be mentioned from here:

1. **Maximum likelihood classification showed a good overall accuracy and fairly acceptable robustness for analyzing peatland vegetation patterns from site to site:** The robustness of MLC in large scale spatial analysis is a big problem. Different color tones between images mostly existed, which was the one of the main factors influencing robustness of MLC. The other one was different spectral signatures of land cover types. An effective way for improving robustness in this study was merging sample points from several peatlands for generating one single signature file for applying to other peatland locations.

2. **Average patch size of hummock showed a downward trend from cold region to warm region and the largest average patch size (of regions) was in cold-moderate temperature (north-central) region:** These results differed from our hypotheses. It was supposed that hummocks would be bigger in warmer areas. That the biggest hummocks (group average) appeared in between end-regions (far north and southernmost) was also unexpected. The latter situation was already discussed in 6.1.2. With regard to the former one, several possible explanations are listed here: 1) The sampling strategy of peatland locations was not great. Several peatland locations were too close to each other (i.e. Peatland 34 with Peatland 35, Peatland 3 with Peatland 4, Peatland 19 with Peatland 20). Then, the representativeness of several peatlands was questionable. 2) The dynamic state of hummock-hollow microform could also be influenced by mire regions. Thus, research on peatland patterning can be based on separate mire regions. 3) There are factors other than evapotranspiration have significant impact on peatland patterning along temperature gradient.

3. **As a whole, hummocks were smaller in wetter regions:** The same as pattern metrics ~ temperature correlation, pattern metrics ~ precipitation was also not significant, as shown in results of regression analysis and pattern metrics ~ precipitation sub-areas boxplots. This finding supported the hypothesis that more hollows appear in wet areas. If precipitation map with higher spatial resolution was provided, then it would be reasonable to divide Sweden into more precipitation sub-areas. Accordingly, clearer trends would be read from boxplots (plotting pattern metrics ~ precipitation sub-areas).

4. **It is possible to apply the alternative stable state theory to peatland patterning change along temperature gradients in Sweden:** Firstly, two peaks in density curves of pattern-metric values were found in every correlogram, which could refer to "stable states" (in alternative stable state theory). Besides, abrupt jumps in values of pattern metrics (relation between pattern metrics and temperature sub-regions) and in values of patterning criteria (patch size and striping in visual assessment) were witnessed between groups, which could indicate transitions between states. However, it should be pointed out that the sample size of peatlands was not big enough to prove the theory. If there are at least hundreds of sample sites, then results will be more convincing. As for precipitation gradient, this study was unable to demonstrate that alternative stable state theory could explain the correlation between pattern metrics and temperature.

8 | Acknowledgements

Foremost, I would like to express my sincere gratitude to my advisors Mr. Lammert Kooistra and Mr. Jelmer Nijp for the continuous support of my major thesis, for their patience, motivation and enthusiasm. Besides, I would like to thank friends who helped me a lot with my thesis during last months: Kaja Hribar, Smriti Tiwari and Vo Thi Minh Hoang for their encouragement, insightful comments. My sincere thank also goes to Timon Weitkamp, for offering me many helps during the first months of my thesis. Feeling gratefully, I would like to thank my family: my mother Jiaodi Peng and my father Kecai Wan, for supporting me to study in the Netherlands.

In addition, it is the first time for me to do a continuous research for more than half year. I felt uncapable of conducting this research in early months. However, I gradually picked up confidence with carrying it on. I also dared not to ask questions to my supervisors before. The great kindness of Mr. Lammert Kooistra and Mr. Jelmer Nijp motivated me to ask more questions and put me back to the track.

Lastly, I want to say thanks to myself, for my perseverance during the last months. I will never forget the day before handing in this report. I spent more than 24 hours on finishing up the final version of report.

9 | Reference

Belyea, L. R. and N. Malmer (2004). "Carbon sequestration in peatland: patterns and mechanisms of response to climate change." Global Change Biology **10**(7): 1043-1052.
Booth, D. and R. Oldfield (1989). "A comparison of classification algorithms in terms of speed and accuracy after the application of a post-classification modal filter." Remote Sensing **10**(7): 1271-1276.
Branfireun, B. A. (2004). "DOES MICROTOPOGRAPHY INFLUENCE SUBSURFACE PORE-WATER CHEMISTRY? IMPLICATIONS FOR THE STUDY OF METHYLMERCURYIN PEATLANDS." Wetlands **24**(1): 207-211.
Breeuwer, A., M. M. Heijmans, B. J. Robroek and F. Berendse (2008). "The effect of temperature on growth and competition between Sphagnum species." Oecologia **156**(1): 155-167.
Bubier, J. L., P. M. Crill, T. R. Moore, K. Savage and R. K. Varner (1998). "Seasonal patterns and controls on net ecosystem CO2 exchange in a boreal peatland complex." Global Biogeochemical Cycles **12**(4): 703-714.
Cline, M., R. Feagin, K. Yeager and J. Van Alstyne (2011). "Fault-induced wetland loss at Matagorda, Texas, USA: land cover changes from 1943 to 2008." Geocarto International **26**(8): 633-645.
Connolly, J. and N. Holden (2017). "Detecting peatland drains with Object Based Image Analysis and Geoeye-1 imagery." Carbon balance and management **12**(1): 7.
CTT. (2018). "Climate of Sweden." from https://www.climatestotravel.com/climate/sweden.
Dang, A., H. Jia and X. Chen (2010). ERDAS IMAGINE Remote Sensing Image Processing Course, Beijing, Tsinghua University Press.
EEA. (2017). "Natura 2000 data - the European network of protected sites." from https://www.eea.europa.eu/data-and-maps/data/natura-9#tab-gis-data.
Eppinga, M. B., M. Rietkerk, W. Borren, E. D. Lapshina, W. Bleuten and M. J. Wassen (2008). "Regular surface patterning of peatlands: confronting theory with field data." Ecosystems **11**(4): 520-536.
Eppinga, M. B., M. Rietkerk, M. J. Wassen and P. C. De Ruiter (2009). "Linking habitat modification to catastrophic shifts and vegetation patterns in bogs." Plant Ecology **200**(1): 53-68.
eXtension.org. (2013, 17/10). "What's the difference between a supervised and unsupervised image classification?".
Folke, C., S. Carpenter, B. Walker, M. Scheffer, T. Chapin and J. Rockström (2010). "Resilience thinking: integrating resilience, adaptability and transformability." Ecology and society **15**(4).
Gaillard, M.-J., S. Sugita, F. Mazier, A.-K. Trondman, A. Brostrom, T. Hickler, J. O. Kaplan, E. Kjellström, U. Kokfelt and P. Kunes (2010). "Holocene land-cover reconstructions for studies on land cover-climate feedbacks." Climate of the Past **6**: 483-499.
Gorham, E. (1991). "Northern peatlands: role in the carbon cycle and probable responses to climatic warming." Ecological applications **1**(2): 182-195.
Gunnarsson, U. and M. Löfroth (2009). The Swedish Wetland Survey.
Guo, M., J. Li, C. Sheng, J. Xu and L. Wu (2017). "A Review of Wetland Remote Sensing." Sensors **17**(4): 777.
Hogland, J., N. Billor and N. Anderson (2013). "Comparison of standard maximum likelihood classification and polytomous logistic regression used in remote sensing." European Journal of Remote Sensing **46**(1): 623-640.
Holden, J. (2005). "Peatland hydrology and carbon release: why small-scale process matters." Philosophical Transactions of the Royal Society of London A: Mathematical, Physical and Engineering Sciences **363**(1837): 2891-2913.
Holmström, H., M. Nilsson and G. Ståhl (2001). "Simultaneous Estimations of Forest Parameters using Aerial Photograph Interpreted Data and the k Nearest Neighbour Method." Scandinavian Journal of Forest Research **16**(1): 67-78.
Holopainen, M. and S. Jauhiainen (1999). "Detection of peatland vegetation types using digitized aerial photographs." Canadian journal of remote sensing **25**(5): 475-485.
IPCC. (2005). "Physical Climate Observation Data." from http://www.ipcc-data.org/observ/clim/cru_ts2_1.html.
Kéfi, S., M. Holmgren and M. Scheffer (2016). "When can positive interactions cause alternative stable states in ecosystems?" Functional Ecology **30**(1): 88-97.
Kleinen, T., V. Brovkin and R. Schuldt (2012). "A dynamic model of wetland extent and peat accumulation: results for the Holocene." Biogeosciences **9**(1): 235-248.
Lehmann, J. R., W. Münchberger, C. Knoth, C. Blodau, F. Nieberding, T. Prinz, V. A. Pancotto and T. Kleinebecker (2016). "High-Resolution Classification of South

Patagonian Peat Bog Microforms Reveals Potential Gaps in Up-Scaled CH4 Fluxes by use of Unmanned Aerial System (UAS) and CIR Imagery." Remote Sensing **8**(3): 173.
Li, Z., W. Wu, X. Liu, B. D. Fath, H. Sun, X. Liu, X. Xiao and J. Cao (2017). "Land use/cover change and regional climate change in an arid grassland ecosystem of Inner Mongolia, China." Ecological Modelling **353**: 86-94.
Linderholm, H. W. and M. Leine (2004). "An assessment of twentieth century tree-cover changes on a southern Swedish peatland combining dendrochronoloy and aerial photograph analysis." Wetlands **24**(2): 357-363.
Lindsay, R., J. Rigall and F. Burd (1985). "The use of small-scale surface patterns in the classification of British peatlands." Aquilo Serie Botanica: 67-79.
Markinfo. (2006). "Length of growing season in Sweden." from http://www-markinfo.slu.se/eng/climate/vegper.html.
Matthews, E. and I. Fung (1987). "Methane emission from natural wetlands: Global distribution, area, and environmental characteristics of sources." Global biogeochemical cycles **1**(1): 61-86.
McHugh, M. L. (2012). "Interrater reliability: the kappa statistic." Biochemia medica: Biochemia medica **22**(3): 276-282.
Miyamoto, M., K. Yoshino, T. Nagano, T. Ishida and Y. Sato (2004). "Use of balloon aerial photography for classification of Kushiro wetland vegetation, northeastern Japan." Wetlands **24**(3): 701-710.
Nijp, J. J. (2015). Fine scale ecohydrological processes in northern peatlands and their relevance for the carbon cycle, Wageningen University.
Ozesmi, S. L. and M. E. Bauer (2002). "Satellite remote sensing of wetlands." Wetlands ecology and management **10**(5): 381-402.
Qian, W. and Y. Zhu (2001). "Climate change in China from 1880 to 1998 and its impact on the environmental condition." Climatic change **50**(4): 419-444.
Racine, M.-J., M. Bernier and T. Ouarda (2005). "Evaluation of RADARSAT-1 images acquired in fine mode for the study of boreal peatlands: a case study in James Bay, Canada." Canadian Journal of Remote Sensing **31**(6): 450-467.
Rietkerk, M., S. C. Dekker, P. C. De Ruiter and J. van de Koppel (2004). "Self-organized patchiness and catastrophic shifts in ecosystems." Science **305**(5692): 1926-1929.
Rietkerk, M., P. Ketner, L. Stroosnijder and H. H. Prins (1996). "Sahelian rangeland development; a catastrophe?" Journal of Range Management: 512-519.
Rogan, J., J. Franklin and D. A. Roberts (2002). "A comparison of methods for monitoring multitemporal vegetation change using Thematic Mapper imagery." Remote Sensing of Environment **80**(1): 143-156.
Rydin, H., H. Sjörs and M. Löfroth (1999). "7. Mires." Acta Phytogeographica Suecica **84**: 91-112.
Scheffer, M., J. Bascompte, W. A. Brock, V. Brovkin, S. R. Carpenter, V. Dakos, H. Held, E. H. Van Nes, M. Rietkerk and G. Sugihara (2009). "Early-warning signals for critical transitions." Nature **461**(7260): 53-59.
Scheffer, M., S. Carpenter, J. A. Foley, C. Folke and B. Walker (2001). "Catastrophic shifts in ecosystems." Nature **413**(6856): 591-596.
Scheffer, M., S. Carpenter, J. A. Foley, C. Folke and B. Walker (2001). "Catastrophic shifts in ecosystems." Nature **413**(6856): 591.
Sharp, J. L., R. S. Sojda, M. Greenwood, D. O. Rosenberry and J. M. Warren (2013). "Statistical classification of vegetation and water depths in montane wetlands." Ecohydrology **6**(2): 173-181.
Shukla, J., C. Nobre and P. Sellers (1990). "Amazon deforestation and climate change." Science(Washington) **247**(4948): 1322-1325.
Souza, S. R. d., L. Azulay-Abulafia and L. V. d. Nascimento (2011). "Validation of the commitment index of skin and mucous membranes in pemphigus vulgaris for the clinical evaluation of patients with pemphigus vulgaris." Anais brasileiros de dermatologia **86**(2): 284-291.
Wieder, R. K. and D. H. Vitt (2006). Boreal peatland ecosystems, Springer Science & Business Media.
Wijaya, A., P. Reddy Marpu and R. Gloaguen (2010). "Discrimination of peatlands in tropical swamp forests using dual-polarimetric SAR and Landsat ETM data." International Journal of Image and Data Fusion **1**(3): 257-270.
Yetang, T. F. H. and L. H. L. Xuetian (1997). "A Model for Quantitative Reconstruction of Climatic Change Recorded in Peat Archives." BULLETIN OF MINERALOGY PETROLOGY AND GEOCHEMISTRY: 02.
Zhang, Y., C. Li, C. C. Trettin, H. Li and G. Sun (2002). "An integrated model of soil, hydrology, and vegetation for carbon dynamics in wetland ecosystems." Global Biogeochemical Cycles **16**(4).

Appendix | A *An Overview of Peatland Locations*

Number	Sub-area		Significance	Coordinate (A random point in each peatland)		Area（Natura2000 Subset）/m^2
	Precipitation Sub-area	Temperature Sub-area		Latitude	Longitude	
1	3	5	2	56.668395°	13.250469°	29760238.97
2			1	56.802232°	13.522281°	3597777.36
3			1	56.782421°	14.068587°	3441676.36
4			1	56.833003°	14.093921°	5695690.77
5		4	1	57.496013°	14.248527°	5689584.18
6			1	57.317118°	14.269325°	18796747.62
7			1	58.079715°	12.734417°	5713399.84
8			2	57.268438°	13.146673°	10944417.87
9		3	1	58.274694°	13.390362°	17246507.37
10			1	58.063217°	13.198942°	3891263.11
11			2	60.154662°	13.945120°	17484073.97
12			1	61.096667°	15.533374°	3001680.68
13		2	1	63.282260°	16.429112°	8421404.04
14			1	62.247540°	14.452716°	59038399.66
15			1	62.691379°	15.162451°	4548983.63
16		1	1	64.507206°	17.771912°	70516821.72
17			1	64.669433°	17.612164°	17294959.63
18			1	63.283612°	12.422121°	89545111.84
19	2	5	1	56.312738°	13.506313°	3415595.78
20			1	56.269396°	13.553272°	3101296.31
21			1	56.722636°	14.424915°	3867530.61
22		4	1	58.004896°	13.947173°	3973110.00
23			1	59.010357°	14.458845°	4998423.58
24			1	59.049716°	14.517076°	2887556.07
25		3	1	60.164981°	14.717855°	11066004.45
26			1	60.772144°	16.142971°	1364544.54
27			1	60.898815°	16.075200°	1229105.61
28		2	2	63.692067°	15.536331°	1692394.16
29			1	63.428255°	15.071457°	7469696.01

Number	Sub-area		Significance	Coordinate (A random point in each peatland)		Area（Natura2000 Subset）/m^2
	Precipitation Sub-area	Temperature Sub-area		Latitude	Longitude	
30			1	62.846014°	14.118914°	36258632.22
31		1	2	64.855002°	17.504681°	22922861.08
32			1	65.504999°	19.004643°	42094800.93
33			1	66.081827°	20.330476°	19872010.02
34	1	5	1	56.823497°	15.278220°	6593491.06
35			1	56.837960°	15.309755°	6593491.06
36		4	1	58.434253°	13.785061°	4475512.93
37			1	58.379870°	13.771970°	16827607.69
38			2	58.785067°	15.202596°	2094775.09
39		3	2	60.141082°	16.087235°	1332512.26
40			1	60.311474°	16.939448°	9881692.24
41			1	64.581276°	20.040424°	8377514.44
42		2	1	66.393812°	20.927439°	30280541.57
43			2	66.373712°	22.152578°	1198284.99
44			1	63.344688°	14.410832°	2299185.60
45		1	1	66.500354°	21.716558°	271165128.13
46			1	67.298279°	20.811699°	979961561.99
47			2	65.560136°	18.121936°	10131798.55

Figure A.1.*General information of all of the peatland locations (Sigificance was used for filtering out peatlands with drainage systems or not located in the mire regions of Mountain Mire Region, Palsa Mire Region, Northern Mire Region and Pine bog-marsh Mire Region (Gunnarsson and Löfroth 2009); Significance 1 – matching conditions, Significance 2 – not matching conditions)*

Appendix | B *Examples of Classified Maps*

▲***Figure B*** *(Continue from Figure 5.1) Examples of land-cover classification results of peatlands. The figure consists of a series of graphs, which are named with alphabets from a. For each subgraph, the classified maps of the 1st round classification (RGB image input, 10m-radius buffer surrounding sample points), the 2nd round classification (RGB, IR images and DEM input, 1m-radius buffer surrounding sample points) and original aerial images (RGB band) are shown from left to right.*

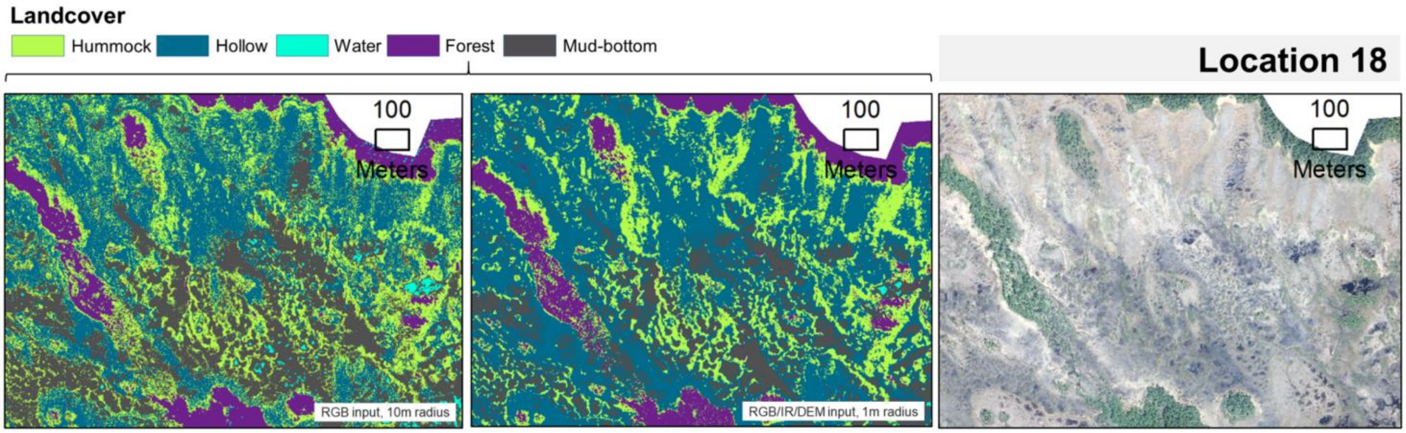

Figure B.1. *Land cover classification results of the representative peatland in group 1 (Peatland 18)*

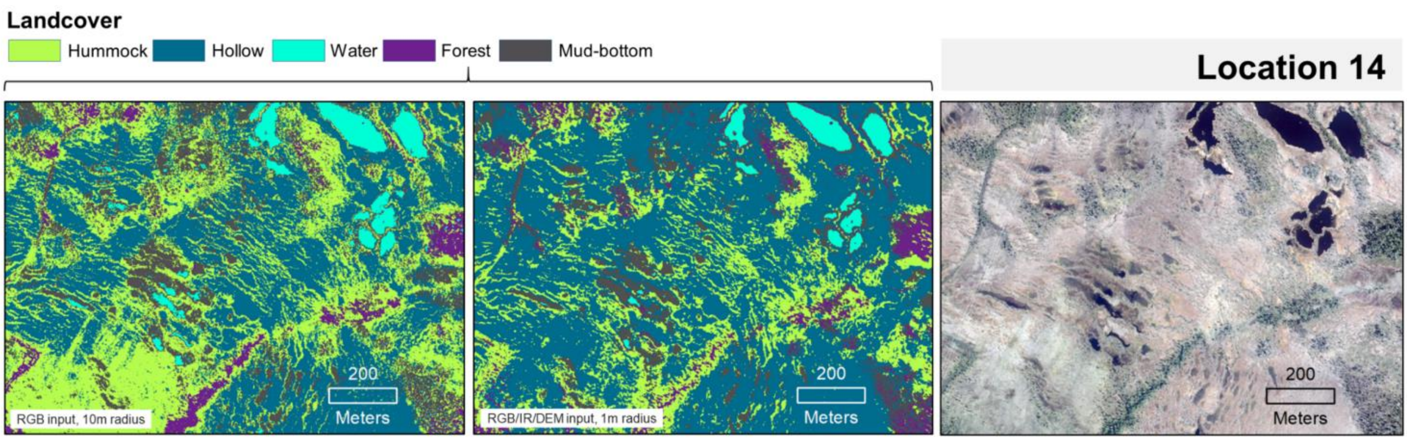

Figure B.2. *Land cover classification results of the representative peatland in group 2 (Peatland 14)*

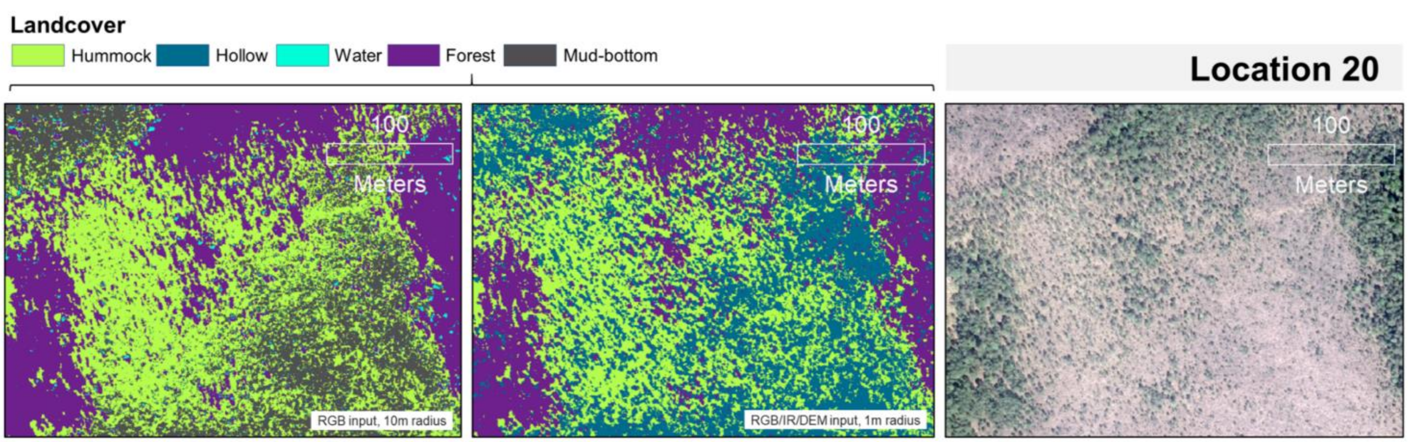

Figure B.3. *An example of land cover classification results of other peatlands (where signature files applied to) in group 5 (Peatland 20)*

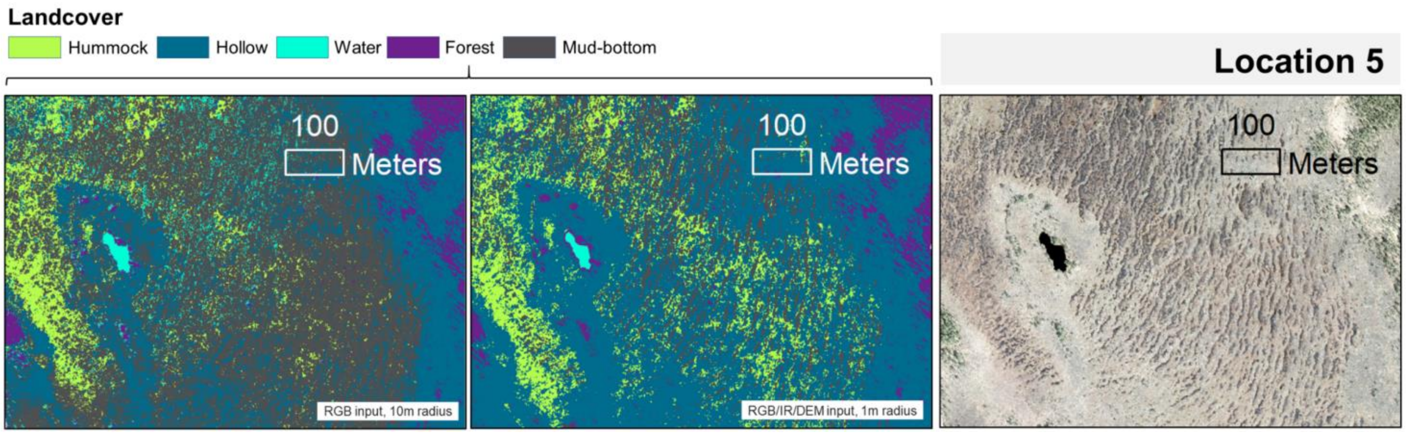

Figure B.4. *Land cover classification results of the representative peatland in group 4 (Peatland 5)*

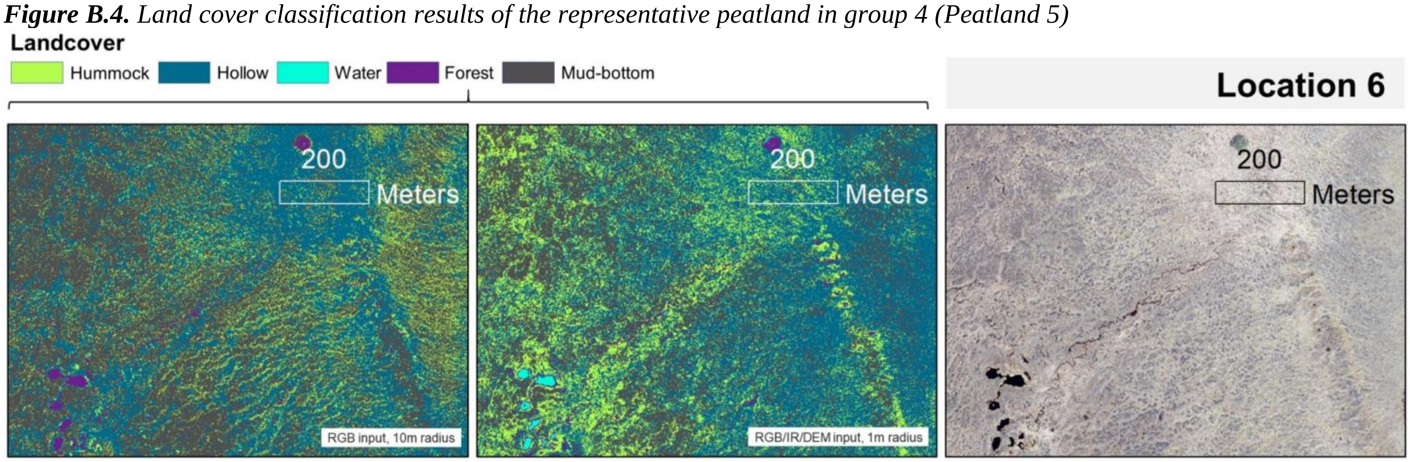

Figure B.5. *An example of land cover classification results of other peatlands (where signature files applied to) in group 4 (Peatland 6)*

Appendix | C *Examples of Visual Assessment*

▲***Figure C*** *The rest of visual assessment results by groups (following Figure 5.2). From left to right in the graphs: peatland number, aerial images of peatlands (in RGB band), hummocks' distribution extracted from classified maps, visual assessment criteria (1) Salt-and-pepper effect in maps of hummocks' distribution, 2) Average patch size of hummocks, 3) (The extent of) striping patterning of hummocks). They are rated form the number of 1 to 5, the legend is shown on the right.*

Peatland number	Aerial imagery (RGB)	Classified map (2nd round)	Visual assessment criteria (1-5 rating)		
			Salt-and-pepper effect	Patch size (Hummock)	Striping
16			4	3	2
17	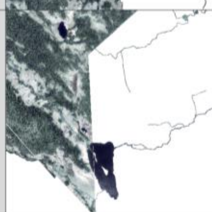	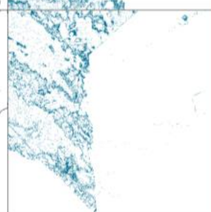	5	2	3
18		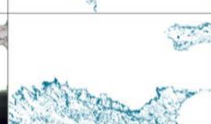	1	2	3
32		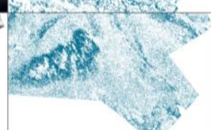	5	2	2
33		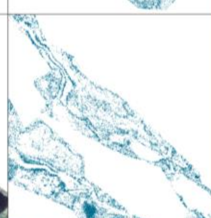	3	2	2
45		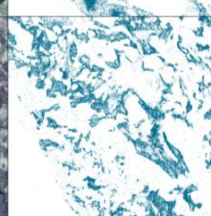	3	4	3
46	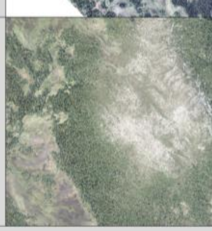	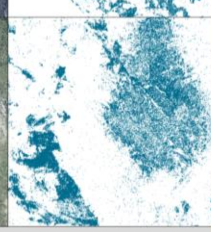	3	4	1
Average			**3.4**	**2.7**	**2.3**

Figure C.1. *Visual assessment result of Group 1 (group under very-low-temperature condition)*

Peatland number	Aerial imagery (RGB)	Classified map (2^{nd} round)	Visual assessment criteria		
			Salt-and-pepper effect	Patch size (Hummock)	Striping
5		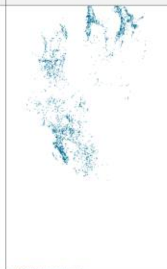	2	1	1
6	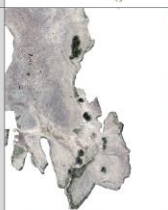	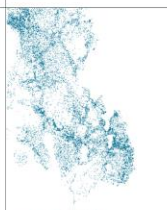	4	2	2
7			4	3	2
22			3	1	1
23		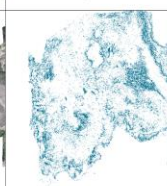	2	3	3
24	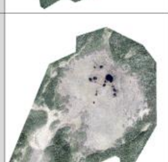	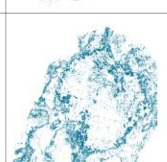	2	3	2
36		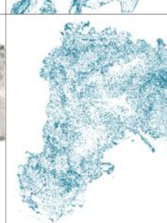	3	3	4
37		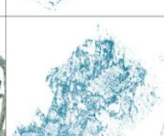	3	3	3
38			2	4	2
Average			**2.8**	**2.6**	**2.2**

Figure C.2. *Visual assessment result of Group 4 (group under high-temperature condition)*

Peatland number	Aerial imagery (RGB)	Classified map (2^{nd} round)	Visual assessment criteria		
			Salt-and-pepper effect	Patch size (Hummock)	Striping
2		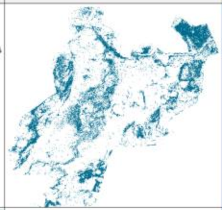	3	3	1
3	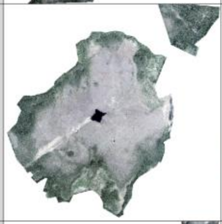	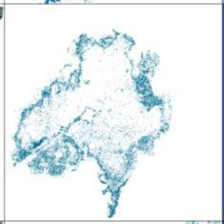	4	1	1
4			5	1	1
19	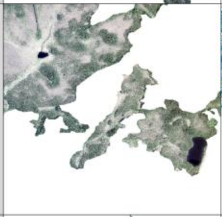	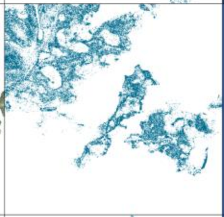	4	4	2
20	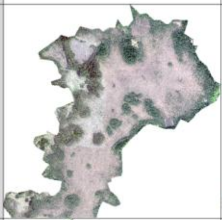	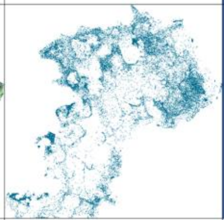	4	2	2
34	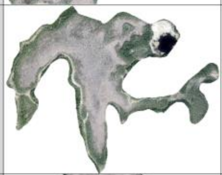	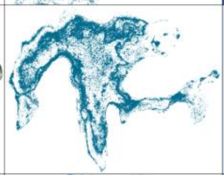	1	4	3
35	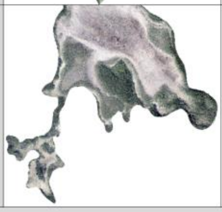	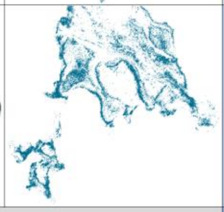	2	3	2
Average			**3.3**	**2.6**	**1.7**

Figure C.3. *Visual assessment result of Group 5 (group under very-high-temperature condition)*

Appendix | D *Confusion Matrices*

Figure D.1.*Confusion matrices of the classification results using the input of RGB image and buffer radius of 10 meters.*

(a) Representative peatland of Group 1: peatland in location 18

Peatland Location 18									
Known Cover Types/ Classification Results			Actual Class					Total	**User's Accuracy**
			1	2	3	4	5		
			Hummock	Hollow	Water	Forest	Mud-bottom		
Predicted Class	1	Hummock	4	2	0	0	0	6	66.67%
	2	Hollow	1	5	0	0	0	6	83.33%
	3	Water	0	0	2	0	0	2	100.00%
	4	Forest	0	0	0	3	0	3	100.00%
	5	Mud-bottom	2	1	0	0	1	4	25.00%
Total			7	8	2	3	1	**21**	
Producer's Accuracy			57.14%	62.50%	100.00%	100.00%	100.00%		**71.43%**

(b) Representative peatland of Group 2: peatland in location 14

Peatland Location 14									
Known Cover Types/ Classification Results			Actual Class					Total	**User's Accuracy**
			1	2	3	4	5		
			Hummock	Hollow	Water	Forest	Mud-bottom		
Predicted Class	1	Hummock	5	0	0	0	1	6	83.33%
	2	Hollow	1	5	0	0	0	6	83.33%
	3	Water	0	0	2	0	0	2	100.00%
	4	Forest	1	0	0	1	1	3	33.33%
	5	Mud-bottom	0	1	0	1	2	4	50.00%
Total			7	6	2	2	4	**21**	
Producer's Accuracy			71.43%	83.33%	100.00%	50.00%	50.00%		**71.43%**

(c) Representative peatland of Group 3: peatland in location 27

Peatland Location 27									
Known Cover Types/ Classification Results			Actual Class					Total	**User's Accuracy**
			1	2	3	4	5		
			Hummock	Hollow	Water	Forest	Mud-bottom		
Predicted Class	1	Hummock	5	1	0	0	0	6	83.33%
	2	Hollow	1	5	0	0	0	6	83.33%
	3	Water	0	0	2	0	0	2	100.00%
	4	Forest	0	0	0	3	0	3	100.00%
	5	Mud-bottom	2	2	0	0	0	4	0.00%
Total			8	8	2	3	0	**21**	
Producer's Accuracy			62.50%	62.50%	100.00%	100.00%	0.00%		**71.43%**

(d) Representative peatland of Group 4: peatland in location 5

Peatland Location 5									
Known Cover Types/ Classification Results			Actual Class					Total	**User's Accuracy**
			1	2	3	4	5		
			Hummock	Hollow	Water	Forest	Mud-bottom		
Predicted Class	1	Hummock	5	1	0	0	0	6	83.33%
	2	Hollow	2	4	0	0	0	6	66.67%
	3	Water	0	0	1	0	1	2	50.00%
	4	Forest	1	0	0	2	0	3	66.67%
	5	Mud-bottom	0	2	0	0	2	4	50.00%
Total			8	7	1	2	3	**21**	
Producer's Accuracy			62.50%	57.14%	100.00%	100.00%	66.67%		**66.67%**

(e) Representative peatlands of Group 5: peatlands in location 34&35 and 2

Peatland Location 34&35									
Known Cover Types/ Classification Results			Actual Class					Total	**User's Accuracy**
			1	2	3	4	5		
			Hummock	Hollow	Water	Forest	Mud-bottom		
Predicted Class	1	Hummock	4	1	0	0	1	6	66.67%
	2	Hollow	2	3	0	0	1	6	50.00%
	3	Water	0	0	0	2	0	2	0.00%
	4	Forest	0	0	0	3	0	3	100.00%
	5	Mud-bottom	2	0	0	0	2	4	50.00%
Total			8	4	0	5	4	**21**	
Producer's Accuracy			50.00%	75.00%	0.00%	60.00%	50.00%		**57.14%**

Peatland Location 2									
Known Cover Types/ Classification Results			Actual Class					Total	**User's Accuracy**
			1	2	3	4	5		
			Hummock	Hollow	Water	Forest	Mud-bottom		
Predicted Class	1	Hummock	5	1	0	0	0	6	83.33%
	2	Hollow	2	4	0	0	0	6	66.67%
	3	Water	0	0	0	2	0	2	0.00%
	4	Forest	0	0	0	3	0	3	100.00%
	5	Mud-bottom	1	0	0	2	1	4	25.00%
Total			8	5	0	7	1	**21**	
Producer's Accuracy			62.50%	80.00%	0.00%	42.86%	100.00%		**61.90%**

Figure D.2.*Confusion matrices of the classification results using the input of RGB image, IR image & DEM and buffer radius of 1 meter.*

(a) Representative peatland of Group 1: peatland in location 18

Peatland Location 18										
Known Cover Types/ Classification Results			Actual Class					Total	**User's Accuracy**
			1	2	3	4	5		
			Hummock	Hollow	Water	Forest	Mud-bottom		
Predicted Class	1	Hummock	6	0	0	0	0	6	100.00%
	2	Hollow	1	5	0	0	0	6	83.33%
	3	Water	0	0	2	0	0	2	100.00%
	4	Forest	0	0	0	3	0	3	100.00%
	5	Mud-bottom	0	0	0	0	4	4	100.00%
Total			7	5	2	3	4	**21**	
Producer's Accuracy			85.71%	100.00%	100.00%	100.00%	100.00%		**95.24%**

(b) Representative peatland of Group 2: peatland in location 14

Peatland Location 14									
Known Cover Types/ Classification Results			Actual Class					Total	**User's Accuracy**
			1	2	3	4	5		
			Hummock	Hollow	Water	Forest	Mud-bottom		
Predicted Class	1	Hummock	6	0	0	0	0	6	100.00%
	2	Hollow	1	5	0	0	0	6	83.33%
	3	Water	0	0	2	0	0	2	100.00%
	4	Forest	0	0	0	3	0	3	100.00%
	5	Mud-bottom	1	0	0	1	2	4	50.00%
Total			8	5	2	4	2	**21**	
Producer's Accuracy			75.00%	100.00%	100.00%	75.00%	100.00%		**85.71%**

(c) Representative peatland of Group 3: peatland in location 27

Peatland Location 27									
Known Cover Types/ Classification Results			Actual Class					Total	**User's Accuracy**
			1	2	3	4	5		
			Hummock	Hollow	Water	Forest	Mud-bottom		
Predicted Class	1	Hummock	5	0	0	1	0	6	83.33%
	2	Hollow	1	5	0	0	0	6	83.33%
	3	Water	0	0	2	0	0	2	100.00%
	4	Forest	0	0	0	3	0	3	100.00%
	5	Mud-bottom	1	1	0	1	1	4	25.00%
Total			7	6	2	5	1	**21**	
Producer's Accuracy			71.43%	83.33%	100.00%	60.00%	100.00%		**76.19%**

(d) Representative peatland of Group 4: peatland in location 5

Peatland Location 5									
Known Cover Types/ Classification Results			Actual Class					Total	**User's Accuracy**
			1	2	3	4	5		
			Hummock	Hollow	Water	Forest	Mud-bottom		
Predicted Class	1	Hummock	6	0	0	0	0	6	100.00%
	2	Hollow	2	4	0	0	0	6	66.67%
	3	Water	0	0	2	0	0	2	100.00%
	4	Forest	0	0	0	3	0	3	100.00%
	5	Mud-bottom	0	1	0	0	3	4	75.00%
Total			8	5	2	3	3	**21**	
Producer's Accuracy			75.00%	80.00%	100.00%	100.00%	100.00%		**85.71%**

(e) Representative peatlands of Group 5: peatlands in location 35 and 2

Peatland Location 35									
Known Cover Types/ Classification Results			Actual Class					Total	**User's Accuracy**
			1	2	3	4	5		
			Hummock	Hollow	Water	Forest	Mud-bottom		
Predicted Class	1	Hummock	5	0	0	1	0	6	83.33%
	2	Hollow	1	5	0	0	0	6	83.33%
	3	Water	0	0	2	0	0	2	100.00%
	4	Forest	0	0	0	3	0	3	100.00%
	5	Mud-bottom	0	0	0	1	3	4	75.00%
Total			6	5	2	5	3	**21**	
Producer's Accuracy			83.33%	100.00%	100.00%	60.00%	100.00%		**85.71%**

Peatland Location 2									
Known Cover Types/ Classification Results			Actual Class					Total	**User's Accuracy**
			1	2	3	4	5		
			Hummock	Hollow	Water	Forest	Mud-bottom		
Predicted Class	1	Hummock	5	0	0	1	0	6	83.33%
	2	Hollow	1	4	0	1	0	6	66.67%
	3	Water	0	0	2	0	0	2	100.00%
	4	Forest	0	0	0	3	0	3	100.00%
	5	Mud-bottom	0	2	0	0	2	4	50.00%
Total			6	6	2	5	2	**21**	
Producer's Accuracy			83.33%	66.67%	100.00%	60.00%	100.00%		**76.19%**

Appendix | E *Some Result of Pattern Analysis*

Figure E.1 *(Continue from Figure 5.4) Scatterplot with density curves, showing the correlation between specific pattern metrics and climatic variables. Colors of points are classified by groups*

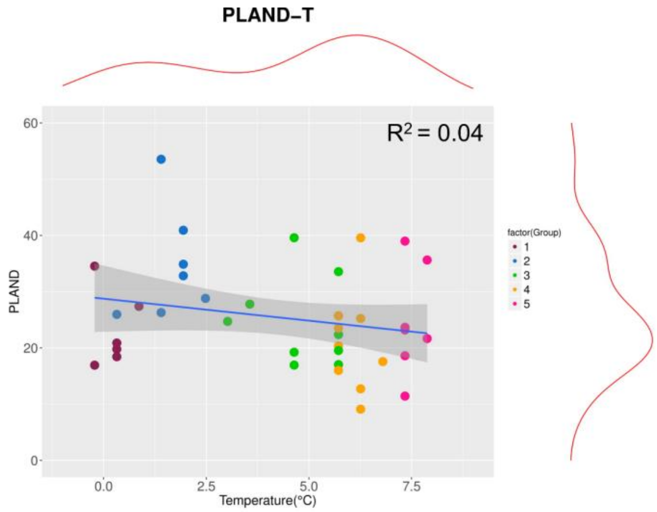

(a) The correlation between the pattern metric of Percentage of Landscape and climatic variable of temperature.

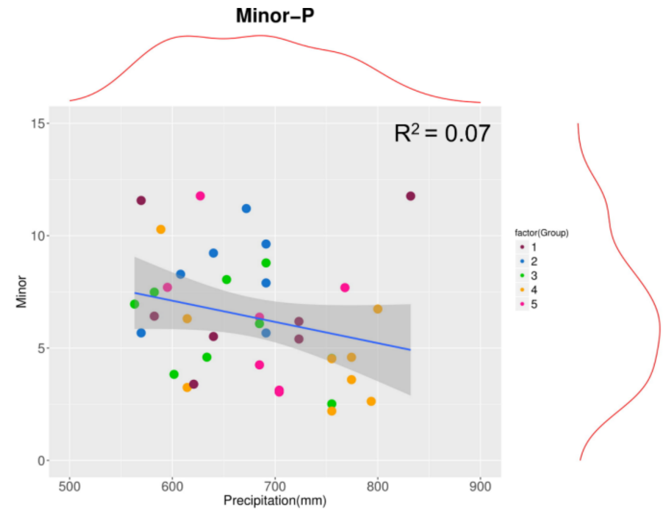

(c) The correlation between the pattern metric of Minor and climatic variable of precipitation.

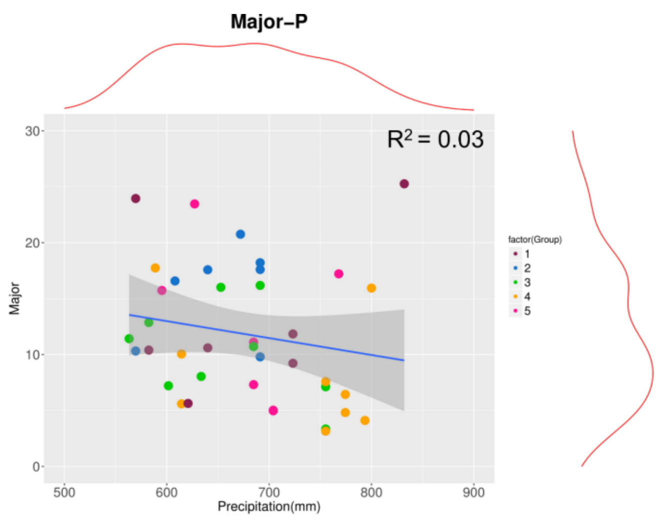

(b) The correlation between the pattern metric of Major and climatic variable of precipitation.

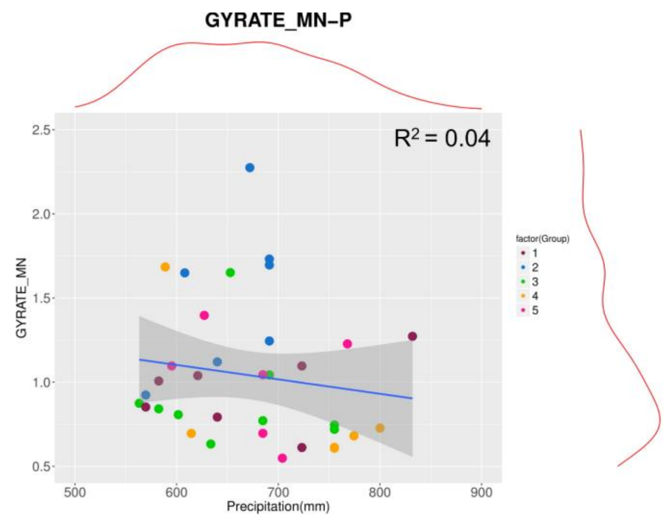

(d) The correlation between the pattern metric of Radius of Gyration-Mean and climatic variable of precipitation.

Table E.1 *Average values of different pattern metrics in peatlands. The corresponding precipitation and temperature values are also shown on the left (P-precipitation, T-temperature).*

Peatland	Group	P	T	Major	Minor	Aniso	GYRATE_MN	PARA_AM	PLAND
2	5	768	7.34	17.21	7.69	0.66	1.23	23307.79	23.20
3	5	704	7.34	5.03	3.13	0.76	0.55	40791.51	18.60
4	5	704	7.34	4.98	3.04	0.70	0.49	46912.19	11.43
5	4	774.4	6.26	6.44	4.59	0.78	0.68	33426.62	12.72
6	4	793.6	6.8	4.12	2.63	0.84	0.47	44447.02	17.56
7	4	800	6.26	15.94	6.74	0.68	0.73	32465.66	25.24
9	3	755.2	5.72	3.35	2.51	0.83	0.72	41704.47	22.37
10	3	755.2	5.72	7.13	4.54	0.80	0.75	35804.42	17.03
12	3	691.2	3.56	16.18	8.79	0.64	1.04	22379.11	27.78
13	2	691.2	1.4	9.80	5.67	0.67	1.24	23296.67	26.28
14	2	672	1.94	20.76	11.21	0.60	2.27	11662.38	32.82
15	2	691.2	1.94	18.21	7.90	0.59	1.73	20701.06	34.88
16	1	723.2	-0.22	11.84	6.18	0.66	1.10	22184.56	34.54
17	1	723.2	-0.22	9.22	5.40	0.70	0.61	34170.72	16.93
18	1	832	0.32	25.26	11.76	0.59	1.27	17675.99	18.43
19	5	684.8	7.88	11.11	6.37	0.69	1.04	19898.53	35.63
20	5	684.8	7.88	7.32	4.25	0.76	0.70	26742.68	21.66
22	4	774.4	6.26	4.82	3.59	0.81	0.49	51168.05	9.10
23	4	614.4	5.72	5.60	3.25	0.72	0.46	40653.84	16.00
24	4	614.4	5.72	10.05	6.31	0.69	0.70	27603.56	20.35
25	3	684.8	4.64	10.72	6.08	0.68	0.77	30651.71	16.94
26	3	633.6	4.64	8.05	4.59	0.71	0.63	37084.08	19.23
27	3	652.8	4.64	16.01	8.05	0.62	1.65	14832.86	39.59
29	2	608	1.94	16.58	8.28	0.63	1.65	18979.32	40.91
30	2	691.2	1.4	17.60	9.63	0.67	1.70	12265.42	53.54
32	1	620.8	0.86	5.64	3.39	0.67	1.04	28621.77	27.39
33	1	640	0.32	10.60	5.51	0.64	0.79	29844.24	20.87
34	5	627.2	7.34	23.46	11.77	0.67	1.40	13951.09	38.98
35	5	595.2	7.34	15.73	7.70	0.64	1.10	19629.80	23.66
36	4	755.2	5.72	3.16	2.20	0.82	0.61	38125.14	23.52
37	4	755.2	5.72	7.58	4.53	0.67	0.61	28728.08	25.70
38	4	588.8	6.26	17.74	10.28	0.66	1.68	21013.91	39.57
39	3	563.2	5.72	11.42	6.96	0.73	0.87	19996.64	33.56
40	3	601.6	5.72	7.22	3.83	0.62	0.81	31096.94	19.54
41	3	582.4	3.02	12.87	7.49	0.64	0.84	28644.63	24.71
42	2	640	0.32	17.58	9.23	0.65	1.12	25922.90	25.96
44	2	569.6	2.48	10.32	5.67	0.68	0.92	26418.48	28.80
45	1	569.6	0.32	23.95	11.57	0.60	0.85	39190.42	19.78
46	1	582.4	-2.38	10.40	6.42	0.74	1.01	29428.68	25.17